UNCLASSIFIED

AD 419022

DEFENSE DOCUMENTATION CENTER

FOR

SCIENTIFIC AND TECHNICAL INFORMATION

CAMERON STATION, ALEXANDRIA, VIRGINIA

UNCLASSIFIED

NOTICE: When government or other drawings, specifications or other data are used for any purpose other than in connection with a definitely related government procurement operation, the U. S. Government thereby incurs no responsibility, nor any obligation whatsoever; and the fact that the Government may have formulated, furnished, or in any way supplied the said drawings, specifications, or other data is not to be regarded by implication or otherwise as in any manner licensing the holder or any other person or corporation, or conveying any rights or permission to manufacture, use or sell any patented invention that may in any way be related thereto.

64-5

CATALOGED BY DDC
AS AD No. 419022

AIR FORCE INSTITUTE OF TECHNOLOGY

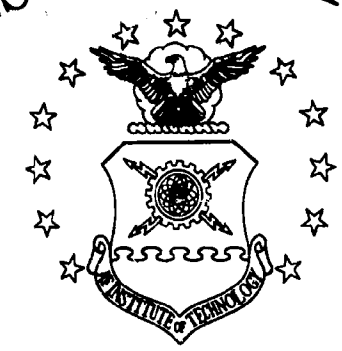

AIR UNIVERSITY
UNITED STATES AIR FORCE

419022

SCHOOL OF ENGINEERING

WRIGHT-PATTERSON AIR FORCE BASE, OHIO

DDC
OCT 8 1963
TISIA A

AF-WP-O-OCT 62 3,500

DETERMINATION OF THE SIZE DISTRIBUTION OF AEROSOLS COLLECTED BY ELECTROSTATIC PRECIPITATION

Capt. Anthony J. Chiota

GNE/Phys/63-5

AF-WP-O-AUG 63 25

DETERMINATION OF THE SIZE DISTRIBUTION OF AEROSOLS COLLECTED BY ELECTROSTATIC PRECIPITATION

THESIS

Presented to the Faculty of the School of Engineering of the

Institute of Technology

Air University

in Partial Fulfillment of the

Requirements fo. the Degree of

Master of Science

by

Anthony Joseph Chiota, B.S.

Captain USAF

Graduate Nuclear Engineering

May 1963

Preface

This report shows the results of my experimental determination of the actual size distribution of aerosols collected by an electrostatic precipitator developed at the Air Force Institute of Technology. The specific precipitator investigated is a model which has evolved over the last two academic years and which has been used for the collection of particulate matter from atmospheric air in the detection of its radioactivity content. The ultimate value of this study is to provide more evidence which would substantiate continued investment of time and funds to perfect an electrostatic precipitator for Air Force field use. The value of such a piece of equipment goes without saying. I feel that the precipitator investigated, on the strength of Baker's work (Ref 1) and the data presented here, warrants continued development towards a working model for field applications.

I wish to thank Captain Charles J. Bridgman, my thesis advisor, for his guidance and help in this project. His enthusiasm and interest in this study has been a constant source of encouragement to me. I would also like to thank Mr. William Schoonover of the Aerial Reconnaissance Laboratory and Major William Metscher of the Electronics Technology Laboratory for providing the necessary space and facilities. I am grateful to Mr. John Blasingame for his generous help in the field of microscopy. I also thank CWO James Miskimen, Staff Sergeant Floyd and Mr. Elworth of the Physics Laboratory and Mr. Winston Wolfe of the AFIT Workshop for their assistance.

Contents

Contents

List of Figures

List of Tables

Dictionary of Variables

Symbol	
AREA	Area of wire holding the corona wires (cm^2).
BETA	Exponent B in equation (5.1) (dimensionless)
CUN(J)	Cunningham correction factor for a particle in size-group J (dimensionless).
CUR	Corona current acting between the corona wires and one plate (amps).
DA	Distance traveled by a particle toward the collection section anode (cm).
DAC	Distance traveled by a particle toward the charging section anode (cm).
DCH	Length of charging section (cm).
DL	Length of collection section (cm).
E	Effective ionization field (volts/cm).
EN	Particle density (particles/cm^3)
ECOL	Electric field in the collection section (volts/cm).
EXPER(J,K)	Number of particles in group J collected at station K, experimentally determined (dimensionless).
FC	Fraction of particles leaving charging section which is collected in the collection section (dimensionless).
FCC	Fraction of particles collected in the charging section (dimensionless).
FQQ	Fraction of bombardment saturation charge achieved by an aerosol in time T (dimensionless).
FRAR	Precipitator frontal area, (cm^2).
FRTC(J,K)	Total fraction of particles in group J collected at collection point K (dimensionless).
G	Ion density (ions/cm^3).
I	Total corona current (amps).

Dictionary of Variables

J	Particle size group (dimensionless).
Q(I)	Charge at any time t (electrons).
QP	Time rate of change of charge dq/dt (electrons/sec).
QQ	Charge achieved by an aerosol as it enters the collection section (electrons).
R(J)	Radius of a particle of size group J (cm).
RR(K)	Radii limits of particle groups (cm).
SEN	Sensitivity of the precipitator (m^3/min).
SEP	Plate separation in the collection section (cm).
SEPC	Plate-grid separation in the charging section (cm).
STN	Station: distance downstream from entrance end of collection plate (cm).
T	Time spent by the aerosol in the charging section (sec).
TDCH	Time a particle spends in the charging section (sec).
TSTN	Time a particle takes to arrive at any station (sec).
u	Micron (10^{-4} cm).
VD	Drift velocity of the aerosol toward the anode in the collection section (cm/sec).
V(I)	Velocity of air flow thru the charging section (cm/sec).
VLCL	Velocity of air flow thru the collection section (cm/sec).
VOL	Volume flow of air thru the precipitator (m^3/min).
n	Kinematic viscosity (ft^2/sec).
XFRTO(J,K)	Fraction of particles in group J collected at station K, experimentally determined (dimensionless).

Abstract

An electrostatic airborne radioactivity collector (EARC-I) is analyzed to determine what correlation exists between the manner in which it actually collects atmospheric aerosols and the theoretical model previously established. Size-distributions of aerosols with radii in the range of 1.0 to 10.0 microns are determined by optical microscopic analysis of particulate matter collected at nine locations along the collection plates of the precipitator. Theoretical size-distributions are calculated for the same locations based on the IBM 7090 solution of theoretical equations describing the charging processes in EARC-I. It is concluded that EARC-I does collect particles roughly in accordance with the theoretical model.

GNE/Phys/63-5

DETERMINATION OF THE SIZE DISTRIBUTION OF AEROSOLS COLLECTED BY ELECTROSTATIC PRECIPITATION

I. Introduction

The purpose of this study is to determine if the electrostatic precipitator, EARC-I, developed at the Air Force Institute of Technology, does in fact collect atmospheric aerosols exactly as predicted by Lamberson (Ref 7) or nearly so. A limited portion of the particle size spectrum is considered. Using the micron, u, as the unit of measurement, the range of consideration includes those particles with a radius equal to 1.0 u up through particles with a radius equal to 10.0 u. The terms: aerosols, particles, particulate matter, dust particles are considered to have the same meaning in this report.

This investigation is experimental in nature. In essence, it consists of collecting particulate matter from the ground-level atmosphere at Wright-Patterson, AFB, Ohio. Samples from the collected matter will be analyzed by optical microscope to determine a particle size-distribution at several locations along the collection plates of EARC-I. Using Lamberson's equations, the theoretical size-distributions will be determined for the same locations. An attempt will be made to explain any discrepancies between the theory and experimental results. Finally, recommendations for future development of EARC-I will be made based upon the experimental findings.

The value of this investigation is in such recommendations. If the theory and experimental data agree within reason, the future development

of EARC-I is justified towards the eventual use by the Air Force as well as by Civil Defense agencies for radioactivity sampling. If, on the other hand, the experimental data indicates that EARC-I produces adequate results on the basis of unexplained phenomena, the continued investigation in this field may not be justified.

Background

The collection and analysis of radioactive aerosols is a project which has been under investigation by graduate Nuclear Engineering students of the Air Force Institute of Technology. A composite theoretical model of the physical processes involved in electrostatic collection was developed by Lamberson (Ref 7). A high volume electrostatic precipitator, EARC-I (Electrostatic Airborne Radioactivity Collector Number 1), was designed, built and used by Baker in his analysis of weapon fallout at Wright-Patterson AFB, Ohio (Ref 1). Stuart (Ref 13) did a design optimization on the basis of the theoretical model.

The feasibility of electrostatic precipitation as a method of collecting radioactive fallout has been demonstrated by Baker. In spite of this, and the long-standing use of electrostatic precipitators for various industrial applications, an examination of the literature relating to this subject indicates that a precise knowledge of the process is lacking. Many of the processes involved are at best described only after a host of simplifying assumptions are made. As a step towards understanding these processes more fully, this thesis investigates the collection of naturally occurring particles in such a precipitator.

II. Apparatus

EARC-I

EARC-I is a two-stage, parallel-plate electrostatic precipitator which is the actual piece of equipment designed and constructed by Baker (Ref 1) in his thesis work. The only work done on the precipitator for this experiment was the replacement of all resistors in the current-limiting network and the rewiring of all grids, making use of the same materials as in the original. So there were no design changes involved. The exact construction details and specifications are available in Bakers thesis (Ref 1:34). Only a brief description and sketch are included here (Figure 2.1).

In the form of a rectangular parallelopiped, EARC-I has two basic sections. The charging section, approximating a line-to-plate geometry, is a wire-to-plane arrangement. The plane is provided by 1/8 inch solid aluminum sheeting. The wire is 0.005 inch diameter tungsten wire tightly drawn across an aluminum frame. In the charging section, there are 17 layers of plate-grid-plate-etc., alternating. It is here that the corona discharge occurs to provide the mechanism for charging aerosol particles. Plate-grid separation is 2.0 cm. Use is made of the negative corona, which means that the grid (wire) is negative with respect to the grounded plate.

The collection section consists of plate-to-plate geometry in the form of 17 horizontally arranged 1/8 inch solid aluminum sheeting at 2.0 cm separation. Nine of the plates in the collection section are

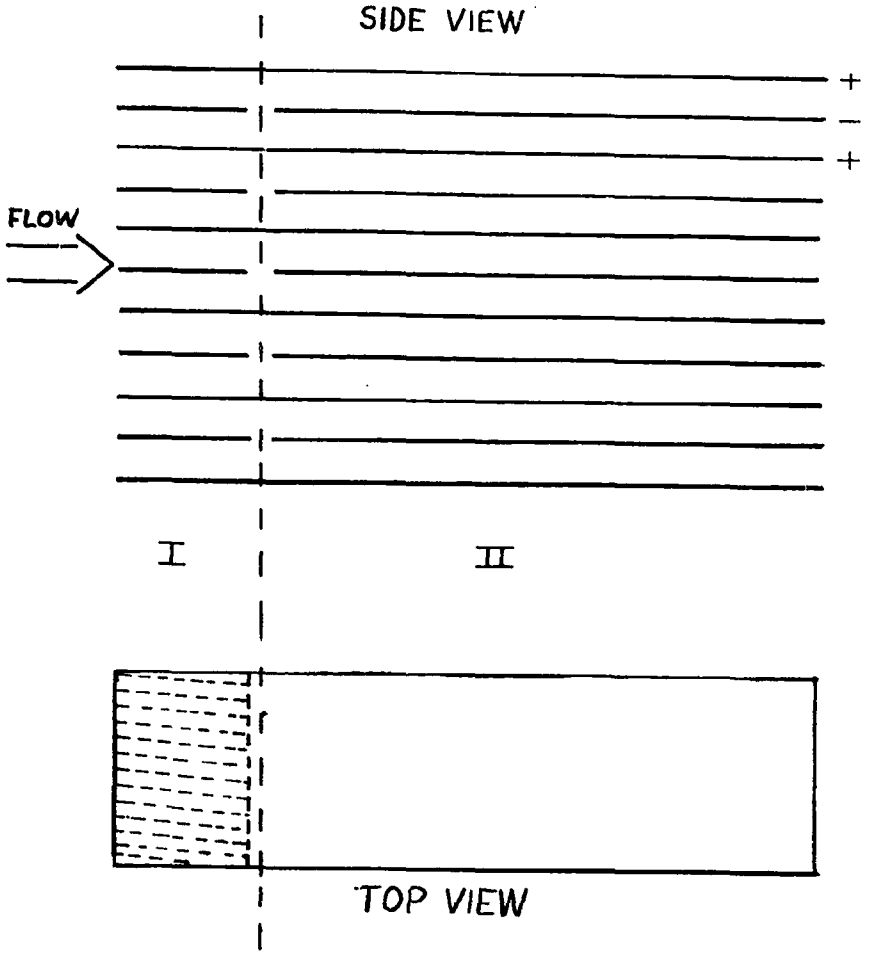

Figure 2.1

Sketch Showing Side and Top Views of Electrode Arrangement in EARC-I (not to scale)

I - Charging Section

II - Collection Section

physical extensions of the plates in the charging section.

Microscope

The microscope used is a Vicker's Projection Microscope manufactured by the Research Laboratories of Messrs. Vickers-Armstrongs, Ltd., York, England. (Figure 2.2)

Lens. The following optical lens were used throughout

a. Objective: Cooke, apochromatic, oil-immersion lens, with 2.2 mm focal length, numerical aperture of 1.32.

b. Projection: Cooke, 15 compensated.

Lighting. For the high magnification used, advantage was taken of the carbon arc lamp available with the Vickers. This provided a high intensity, evenly distributed circular light source. The lamp condenser is mounted close to the carbon arc. Adjustment is provided by an adjustable iris diaphragm for controlling the aperture of the lens. The lens can also be made to slide toward or away from the light source. Figure 2.3 shows the image forming system. The working image was projected on the ground glass projection screen. The screen had a working field etched with a 10 cm x 10 cm area which was further subdivided into 1 cm squares.

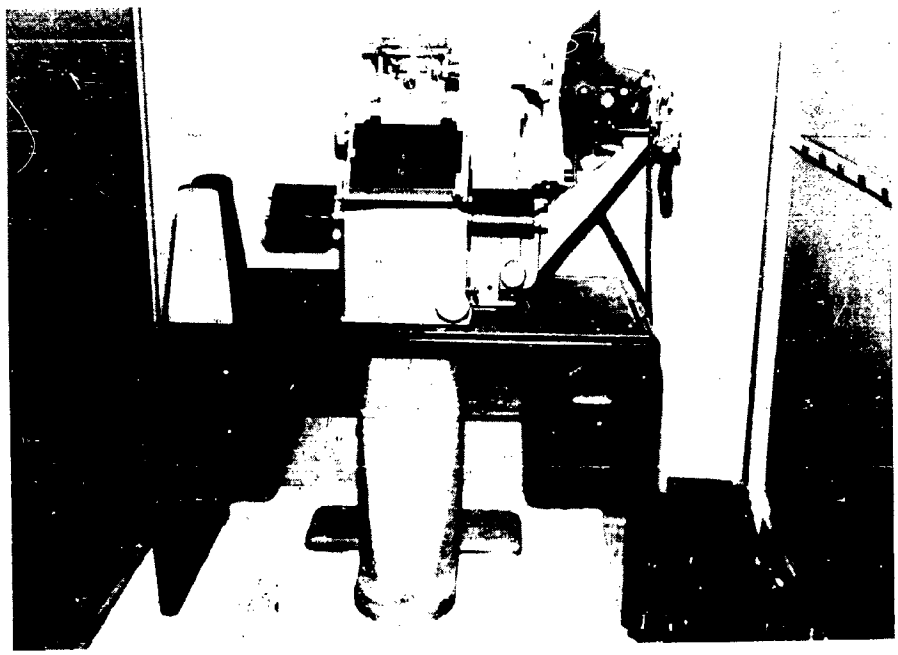

Figure 2.2

Vicker's Projection Microscope

1. Ground-Glass Projection Screen
2. Carbon Arc Lamp

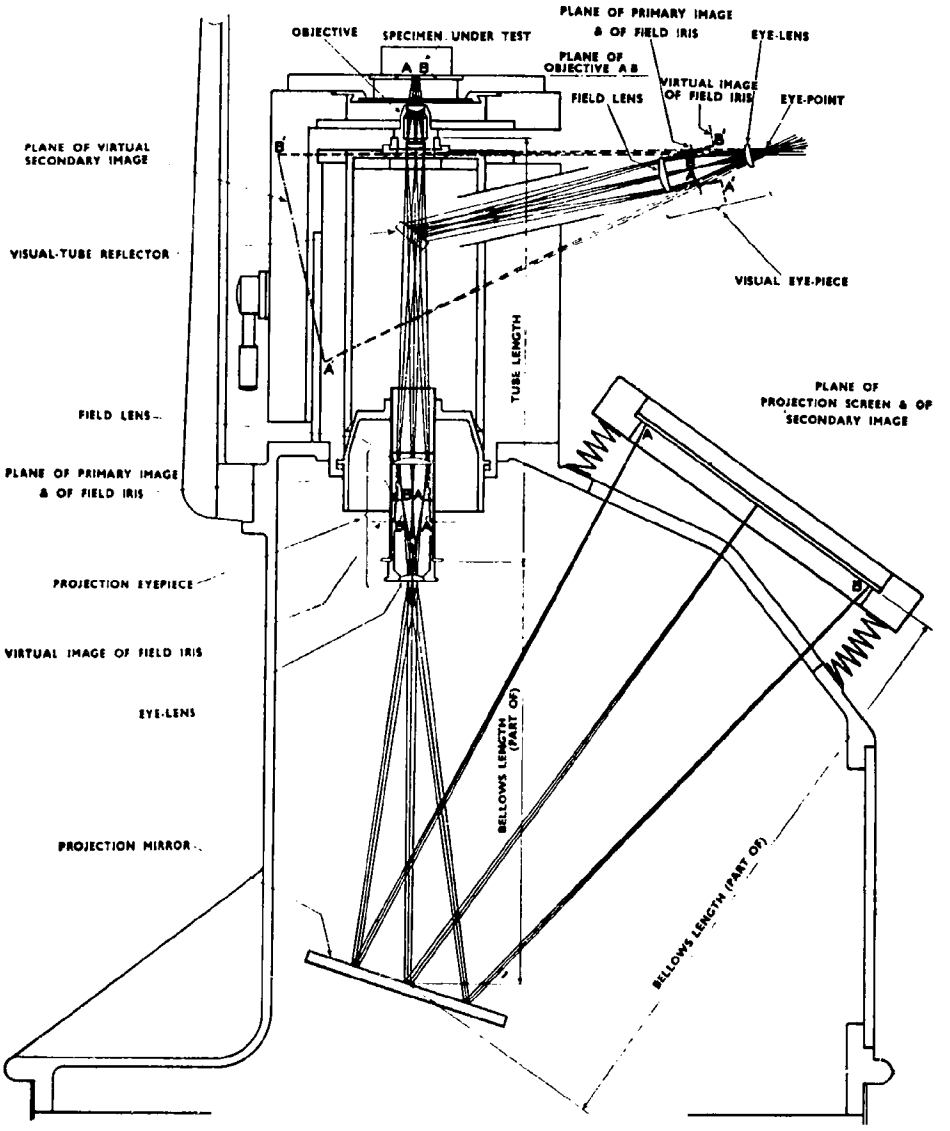

(Ref 17:51)

Figure 2.3

Image-Forming System of Vickers

Projection Microscope

III. Theory

General

The theory which formed the basis for the realization of EARC-I, although presented by Lamberson (Ref 7), is in general agreement with other well-known investigators in this field, e.g. White, Lowe, Lucas, Penney. The chronological sequence of processes involved are briefly stated, then explained in more detail. Figure 3.1 should be an aid in visualizing the processes as they are discussed.

Sequence of Events. Air, which carries minute dust particles, is forced into the precipitator by some device such as a fan or by the forward motion of an aircraft-mounted version of EARC-I. After proceeding some few centimeters into the entrance, the air then enters the charging section. Here, ionized air caused by a corona discharge, imparts a negative charge to the aerosols present in the airstream. The particles, during and after their accumulation of charge, are drawn in accordance with Coulomb's law to grounded collection plates which act as anodes.

Corona Discharge

It will be shown that the swiftness with which a particle is collected depends initially upon the amount of charge it acquires. The source of the charging process is the corona discharge. The corona may be defined as that electrical state which exists between two bodies, the potential between which is sufficiently below the potential required for a generalized breakdown (sparkover) of the dielectric between them. For example, when a potential difference is applied between two parallel plates in air, there is a uniform field present. Increasing the field potential is possible

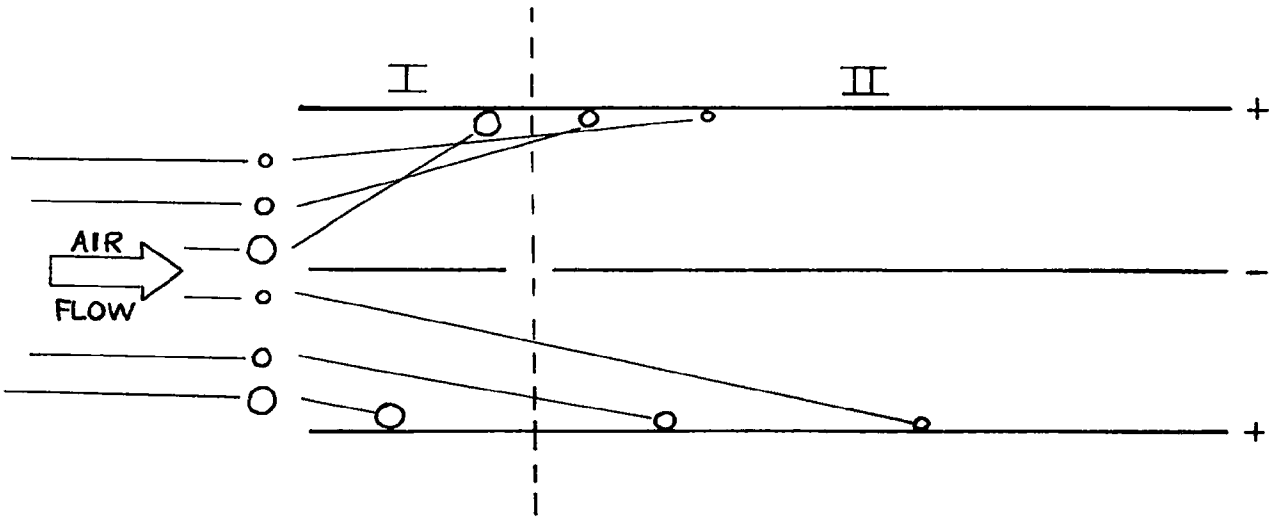

Figure 3.1

Conceptual Sketch Showing Relative

Deposition of Particles as a

Function of Particle Size

I - Charging Section

II - Collection Section

until it reaches approximately 30 KV/cm which is the electrical breakdown point for atmospheric air.

A non-linear electric field is necessary for a corona discharge to occur. Consider two electrodes: a point for the cathode and a plane for the anode. Application of a potential across the electrodes causes a field which has a high value at the point and a lower value at the plane. By applying the proper potential difference, electrical breakdown will occur in the gas close to the point. This localized breakdown constitutes the corona discharge which is necessary to the charging process. A further increase in potential would result in generalized breakdown, effectively short-circuiting the electrodes.

Considering the electrodes found in EARC-I, it can be seen that a potential across the wires and plates will result in a localized electrical breakdown in the air surrounding the wire. Since the wires are the cathodes, it can be visualized that there are two distinct electrical zones in the space between the electrodes. Immediately surrounding the negative wire, positive ions tend to congregate; while the remaining space, and by far the major portion, is occupied with negative ions in transit towards the grounded collection plate. Corona discharge in EARC-I occurs for total ionization current as high as 20 ma at a charging potential of 23 KV (Ref 1:39). Exceeding these limits usually results in complete breakdown (sparkover).

Particle Charging Mechanisms

Bombardment Charging. In bombardment charging the ions formed by the corona move along the lines of force of the electrical field between

the cathode and anode. Upon collision with an aerosol traveling with the air stream, charge is transferred to the aerosol. As the particle charge increases, a sufficiently high Coulombic repulsion to other ions is reached which prevents the further transfer of charge to the particle. At this point, the particle is said to hold a saturation charge. The following assumptions were made to arrive at a mathematical expression to solve for the saturation charge acquired by a particle (Ref 16:1187):

1. The aerosol particles are spherical.

2. Particle diameter is much less than the distance between particles in the airstream.

3. The immediate region surrounding a particle has a uniform ion concentration and electric field.

The assumption made here as well as any other assumptions made in the theoretical development of EARC-I will be discussed later in the light of how they effect the experimental results obtained in this study.

The expression for saturation charge acquired by an aerosol by bombardment charging is (Ref 7:35).

$$q_o = \left[1 + 2\left(\frac{K-1}{K+2}\right)\right]\frac{Er^2}{e} \qquad (3.1)$$

where q_o = saturation charge on particle (electrons)

K = dielectric constant of the aerosol

E = electric field in the charging section (statvolts/cm)

r = particle radius (cm)

e = Electronic charge (esu)

It can be seen that for a given materiel, the saturation charge is

directly proportional to the radius squared and the electric field.

Diffusion Charging. Charging by this method is the result of the thermal motion of ions. Charge is imparted to the aerosol during random collisions with ions. Diffusion charging is dependent upon the particle size, air temperature and the time the particle spends in the charging section. The expression for diffusion charging is (Ref 7:41).

$$q = \frac{rkT}{e^2} \ln\left(1 + \frac{\pi U e^2 r n t}{kT}\right) \qquad (3.2)$$

where q = particle charge (electrons)

U = rms thermal velocity (cm/sec)

n = ion density (ions/cm^3)

r = particle radius (cm)

e = electron charge (esu)

k = Boltzmann constant

T = temperature ($^\circ$K)

t = time (sec)

The assumptions made for the derivation of equation (3.2) are the same as for the derivation of the bombardment charging equation. In addition it was assumed:

4. All ions which reach the particle are attached to it.

Combining Diffusion and Bombardment Charging. The total saturation charge from both charging mechanisms considered is not simply the addition of the charges acquired by each. The differential expression combining both mechanisms follows (Ref 7:43):

$$\frac{dq}{dt} = A - Bq + Cq^2 + De^{-Jq} \qquad (3.3)$$

where $A = 11.16\, nr^2E$

$B = 1.61 \times 10^{-6}\, n$

$C = 5.79 \times 10^{-14}\, n/r^2E$

$D = 15.7 \times 10^{4}\, nr^2$

$J = 5.56 \times 10^{6}/r$

n = ion density

e = base of natural logarithms

Equation (3.3) is a non-linear differential equation which was solved using the IBM 7090 Digital Computer (Ref 13:88). A discussion of the computer solution is presented in Chapter V which covers theoretical predictions of EARC-I performance.

Collection of Charged Particles

Although EARC-I is a two-stage precipitator, collection of charged aerosols is not restricted exclusively to the collection section. As soon as a given particle enters the charging section it immediately begins accumulating negative charge. Simultaneously it feels an attractive force from the grounded plates. A charged particle then, is under the influence of two simultaneous forces at all times during its presence in the precipitator. There is the force of the airstream in which it is traveling. There is also the Coulombic attraction from the oppositely charged collection plates. An expression for evaluating the particle's component of velocity normal to the airstream flow can be derived from two basic principles:

1. Stoke's law describing the motion of a small sphere in a viscous medium

$$F = 6\pi\eta V_o \tag{3.4}$$

where F = drag on particle (dynes)

n = viscosity of air in poise

v_o = terminal velocity of particle in cm/sec

r = particle radius in cm

2. The electrostatic force on a charged particle

$$F = q e E \tag{3.5}$$

where E = field strength (statvolts/cm)

e = charge on the electron (esu)

q = charge on particle (electrons)

Assuming that the particle attains terminal velocity instantaneously; equating equations (3.4) and (3.5); and solving for terminal velocity, one gets

$$V_o = (\text{CONSTANT})\, q E/r \tag{3.6}$$

which is in the direction determined by the field and the charge on the particle. For EARC-I, airflow is parallel to the collection plates which are mounted horizontally. Therefore, V_o will be in a vertical direction. For particles with radii less than 1.5 u, there is an increased probability that they will pass between air molecules. This would result in a higher velocity than is indicated strictly on the basis of charge acquired. The Cunningham correction factor, CUN, compensates for this phenomenon

$$CUN = 1 + \frac{9.42 \times 10^{-6}}{r}\left(1.23 + 0.41 e^{-0.934 \times 10^{-5} r}\right) \qquad (3.7)$$

The corrected drift velocity, v_d, is the product of the particle's terminal velocity and the Cunningham correction factor

$$v_d = v_o \times CUN \qquad (3.8)$$

Typical values of CUN and v_d are shown in Table 3-1. Although Table 3-1 includes particles with radii smaller than those considered in this study, it is interesting to note that for very small particles, the drift velocities are greater than particles with larger radii. This is contrary to what one would expect from the discussion thus far.

Table 3-1

Typical Values of Cunningham Correction Factors, Drift Velocities and Charge as a Function of Radius

Radius (μ)	CUN	V_d (cm/sec)	Charge (electrons)
.125	2.02	3.21	16
.20	1.61	2.80	28
.30	1.39	2.65	46
.425	1.26	3.09	84
.6	1.19	4.18	169
.85	1.14	5.65	340
1.25	1.09	7.95	734
2.0	1.06	12.4	1880
3.0	1.04	18.3	4240
4.25	1.03	25.5	8490

(Ref 7:72A)

IV. Experimental Procedure

The basic test for judging how closely EARC-I operates to the theoretical model was a comparison of the size-distribution of particles collected during actual operation versus the sizes predicted. It remained to collect samples of particulate matter actually precipitated from the atmosphere; then to make a particle size-distribution determination on those samples. This chapter discusses the procedures used.

Collection of Samples

There are many methods for determining the size-distributions of particles in a sample of matter. Examples are sieving, sedimentation, elutriation and centrifuging methods. When applied to the investigation of EARC-I, each of the methods listed has some objectionable disadvantage. Each of the indirect methods involves first collecting particulate matter on the collection plates then devising some method of removal from the plates for the actual sizing procedure. It was reported by Baker (Ref 1:44) that removal of collected particles is a difficult problem. At best, the intermediate step of removing precipitate from the plates would involve loss and/or distortion of the original particles. The direct sieving method would offer the least objectionable method of taking samples of collected aerosols. However, sieving would necessarily introduce obstructions to air flow or perturbations of the electrical fields.

Microscopic analysis seemed to offer the best method of examining collected particles as they were actually precipitated. The use of a microscope was also indicated by the heterogeneity of the particles

contained in atmospheric air. For example, a sedimentation process would doubtlessly dissolve some particles, while the light extinction method of size analysis would be invalid for the wide range of densities found in natural aerosols.

The first consideration then was to collect the particle samples in such a way as to minimize physical and chemical changes from their deposited state. Accordingly, it was decided to use household aluminum foil as the collection surface. The foil was tightly stretched across the surface of the collection plates and taped along the edges to minimize geometrical deviation from a plane surface. There was no visible adverse effects apparent during operation of EARC-I as a result of the foil.

The collection laboratory (Figure 4.1) was on the ground floor of a two-story building. Air was drawn from a 20 ft. x 40 ft. open courtyard in the center of the building and was exited through an external wall fifty feet away. The entrance to EARC-I is a six-foot-long rectangular duct which passed from the courtyard through the laboratory wall. A 90° duct elbow is installed on the outside end of the duct and is fitted with a 1/2 in. wire screen to keep out large objects. A gelman thermal anemometer is mounted in the exhaust duct to measure the speed of the airstream.

Foils were exposed to the precipitation process for different time intervals in order to get a sample with an optimum density of particles deposited for microscopic viewing. The foil exposed for one hour appeared to give the best density for that purpose.

After a precipitation run, samples were taken immediately following shut-down. At measured distances from the entrance end of the collection

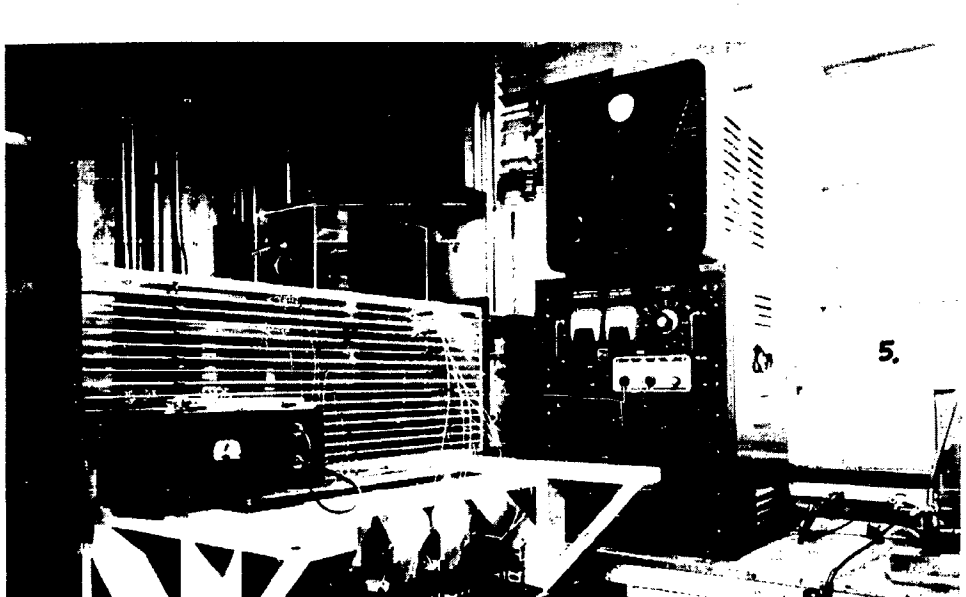

Figure 4.1

Arrangement of Collection Laboratory

1. Exit Duct from EARC-I
2. EARC-I
3. Inlet Duct to EARC-I
4. Power Supply for EARC-I
5. Courtyard

plate (taken as station 0), 0.17 mm-thick cover-glasses were taped to the aluminum foil. The microscope samples were removed by cutting around the coverglass, removing the foil and coverglass together. Samples were arbitrarily taken at nine collection points. A collection point is defined as the width of the coverglass minus the distance of the coverglass along its edges covered by the tape used to secure it to the foil. Table 4-1 shows the stations included by each collection point.

Microscopic Analysis

Since the samples to be analyzed were collected on aluminum foil, it was necessary to use incident lighting for viewing. The best available instrument for this type of work was the Vickers Projection Microscope described earlier.

Magnification. For the size range of interest in this study it was necessary to use the highest magnification available with an optical system. This implied the use of oil immersion lens. The objective lens used throughout the analysis was the 2.2 mm focal length lens. The projection eyepiece was a 15X compensated lens with the mechanical tube length set at 230 mm length. The bellows length, which determines the magnification of the image projected on the ground glass screen, was set on the 90 cm position. (See Figure 2.3).

The lens system (which is taken to mean the object lens, projection lens, mirror, and projection screen) was calibrated against a Bausch and Lomb object micrometer. The micrometer scale was projected through the lens system on to the screen. With the microscope arranged as described above, the smallest division on the micrometer known to be 0.01 mm, measured 50.26 mm $\pm$ 1.005 mm. The magnification then was approximately 5000X.

Table 4-1

Designation of Collection Points

Collection Point	Inclusive Stations (cm)
1	0.1 - 2.1
2	5.5 - 7.5
3	8.0 - 10.0
4	12.0 - 14.0
5	15.0 - 17.0
6	18.0 - 20.0
7	21.5 - 23.5
8	25.0 - 27.0
9	30.0 - 32.5

Microscopic Measurement. There are several methods of taking the actual measurement of particles in a field of view. Among these are measurement by direct observation, projection on a screen and photography. As noted above, the Vickers has facility of projecting the image on a ground glass screen for greater magnification. This is sometimes referred to as "empty magnification", but for the purposes of sizing in the range of interest here, the increased magnification is validly used. The actual measurement consisted of measuring the Martin statistical diameter (to be defined) in all measurements. (See Figure 4.2). A pair of dividers was used to measure the projected particle diameter on the screen. The spread of the dividers was then measured against a plastic centimeter ruler whose smallest division was a millimeter. This method is analogous to the use of the camera lucida for measuring particle sizes. Basically the camera lucida is a way of projecting a magnified image onto a piece of paper where it is traced for subsequent measurement. (Ref 2:70). Within human error measurements were read to the nearest 0.25 mm on the ruler when measuring the spread on the dividers.

Small Particle Statistics. Statistics as applied to small particles is a specialized topic which is most thoroughly treated by Herdan (Ref 3). At the outset of a microscopic analysis, one must reconcile himself to the fact that he is literally looking at a "drop in the ocean". Nonetheless the procedures of microscopy are longstanding and have evolved as valid methods for representing the macroscopic world by investigating a relatively very small sample.

Two of the more common statistical diameters used when measuring

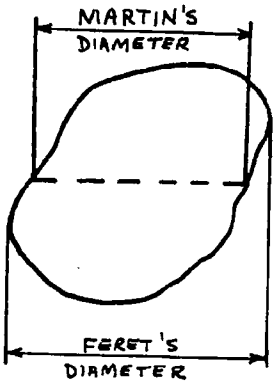

Figure 4.2

Particle Showing Statistical Diameters

particle sizes are Martin's diameter and Feret's diameter (Figure 4.2). Martin's diameter is defined as the chord which bisects the area of the image presented by a particle when viewed through a microscope. The bisecting line is always taken parallel to a fixed direction to avoid introducing bias in the selection of any measured diameter. Feret's diameter is the mean chord perpendicular to two opposite tangents to the particle outline. The tangents are also drawn in some arbitrarily chosen direction. In this study, the Martin statistical diameter was measured, taken in the horizontal direction. It has been shown that of the two, Martin's diameter has less error than Feret's diameter when considering particle surfaces and when compared to the Stoke's diameter (Ref 3:46).

The next logical aspect of arriving at a valid statistical size distribution is the size of the sample analyzed. There are varying opinions on this score. DallaValle indicates that for most measurements, a sample of 200 particles is sufficient to get a valid representation (Ref 2:69). Herdan recommends that the sample contain between 300 and 500 particles (Ref 3:47). Table IV in Skinner, et al (Ref 12:9) gives the minimum number of particles to count for a probable error of 2% as 400. It was therefore decided that a valid representation of the size distributions of the samples taken from EARC-I would result from counting at least 400 particles in each sample. To avoid bias, all particles in a given field of view were counted.

An important assumption which has been implicit in the discussion of the analysis of EARC-I samples should be stated here. It is assumed that what appears as a particle under the microscope i.e. a unit of matter whose

cohesive forces have maintained its viewed size and shape is and was an aerosol originally carried in the airstream being drawn through the precipitator. There is the possibility that an original aerosol upon entering the precipitator could have been altered in size, shape or chemical consistency. Such changes could have occurred in the high electric field in the charging section or upon impact with the collection plate when deposited. There is also the possibility that what appears as a particle is really an aggregate of many smaller particles.

Designation of Particle Groups. It would be meaningless to treat each particle measured in a class by itself. It therefore becomes necessary to group arbitrarily, particles within certain size limits. Table 4-2 lists the particle groups for the purposes of this study and also the average radius of each group. It is necessary to use an average radius in the computer program used to make theoretical calculations.

Use of a Particle Size Analyzer

An attempt was made to extend the range of particles analyzed during this study. For this purpose, use was made of a Particle Size Analyzer (PSA) (Figure 4.3) made by the Southern Research Institute for the U. S. Public Health Service. The PSA was designed to measure particle size-distributions in atmospheric aerosols and in other suspensions of solid particles and liquid droplets in gases (Ref 18:1). It covers the range of particle sizes from 0.15 to 2.0 microns diameter.

EARC-I was modified (Figure 4.4) to permit monitoring "grab samples" of the airstream with PSA. To accomplish this, 1/2 inch holes were drilled

Table 4-2

Designation of Particle Groups by Radii

Group	Inclusive Radii (u)	Average Radius, R(J), (u)
1	$1 \leq R < 2$	1.5
2	$2 \leq R < 3$	2.5
3	$3 \leq R < 4$	3.5
4	$4 \leq R < 5$	4.5
5	$5 \leq R < 6$	5.5
6	$6 \leq R < 7$	6.5
7	$7 \leq R < 8$	7.5
8	$8 \leq R < 9$	8.5
9	$9 \leq R < 10$	9.5

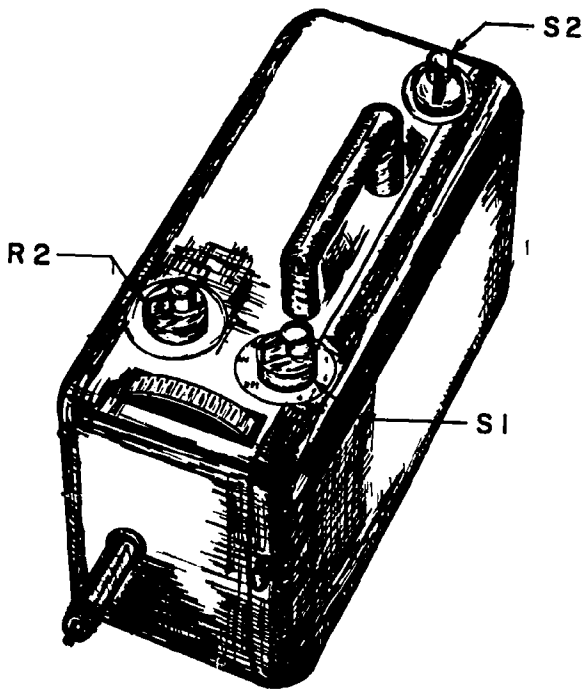

Figure 4.3

Particle Size Analyzer (PSA)

S1 - Selector Switch

S2 - On-Off-Calibration Switch

R2 - Descriminator Potentiometer

(Ref 18)

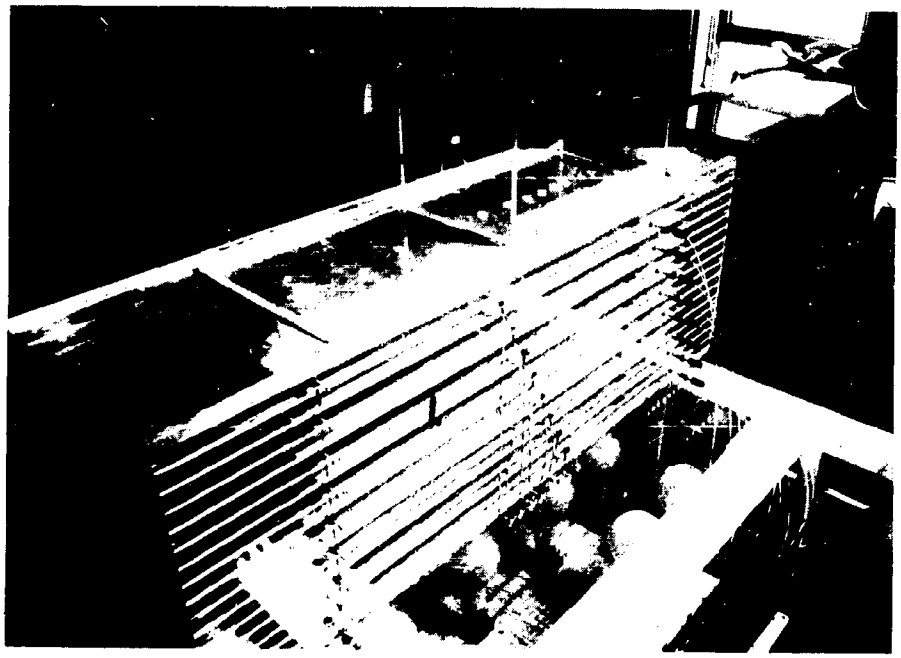

Figure 4.4

EARC-I Modified for Use with PSA

1. EARC-I
2. Plexiglass Container

in the first collection plate (Figure 4.5) at the same collection points at which samples were collected previously for the microscopic analysis. A plexiglass container (Figure 4.6) was constructed to capture the grab samples for monitoring. By making a size-distribution determination at successive collection points, it was hoped to arrive at data similar to that which resulted from the microscopic analysis performed for the range of larger particles.

The attempt was unsuccessful, however. It was found that the PSA was adversely effected by the electric fields in EARC-I. As the power-supply voltage was increased from zero volts, the PSA meter began to give erratic readings. For a total current of 0.2 ma and above, the meter read off-scale. One further attempt was made to make size-distribution measurements of the air immediately before its entrance into EARC-I and immediately after its leaving. Measurements at both locations resulted in meaningless data. It appeared that the high velocity of the airstream caused the PSA to give erratic readings. Additionally, at the exit of EARC-I, the same effect as noted above was observed when the applied voltage was increased from zero volts.

These results, although unsuccessful, are included as possible information for other investigators in this area.

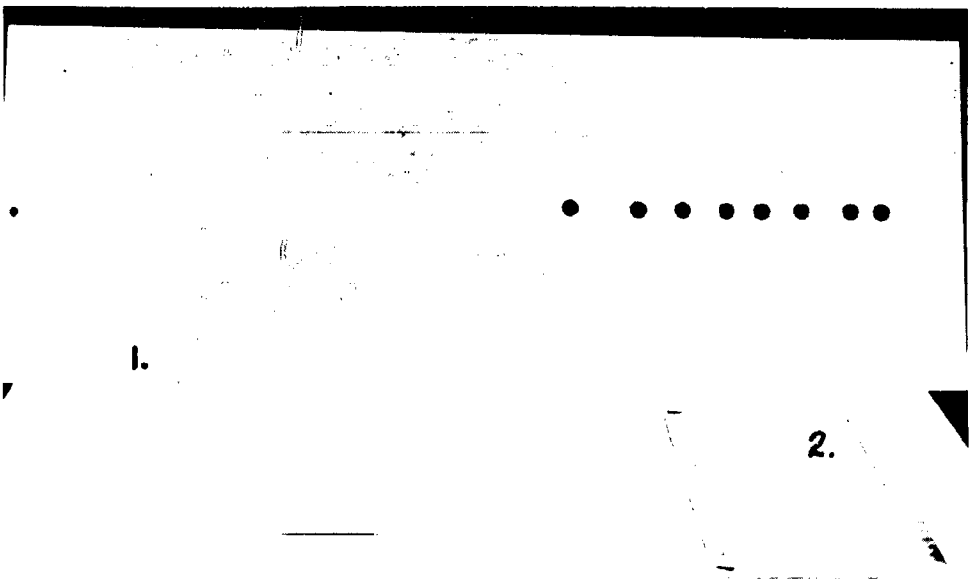

Figure 4.5

1. Collection Plate Modified for Use with Particle Size Analyzer (PSA)

2. Grid from Charging Section of EARC-I

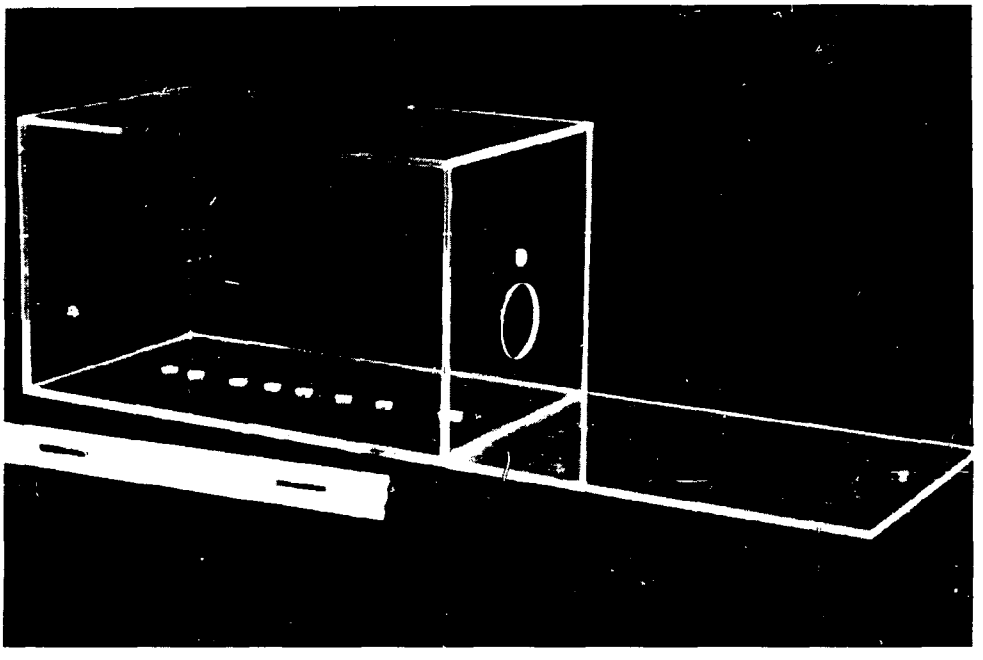

Figure 4.6

Plexiglass Container for Use With PSA

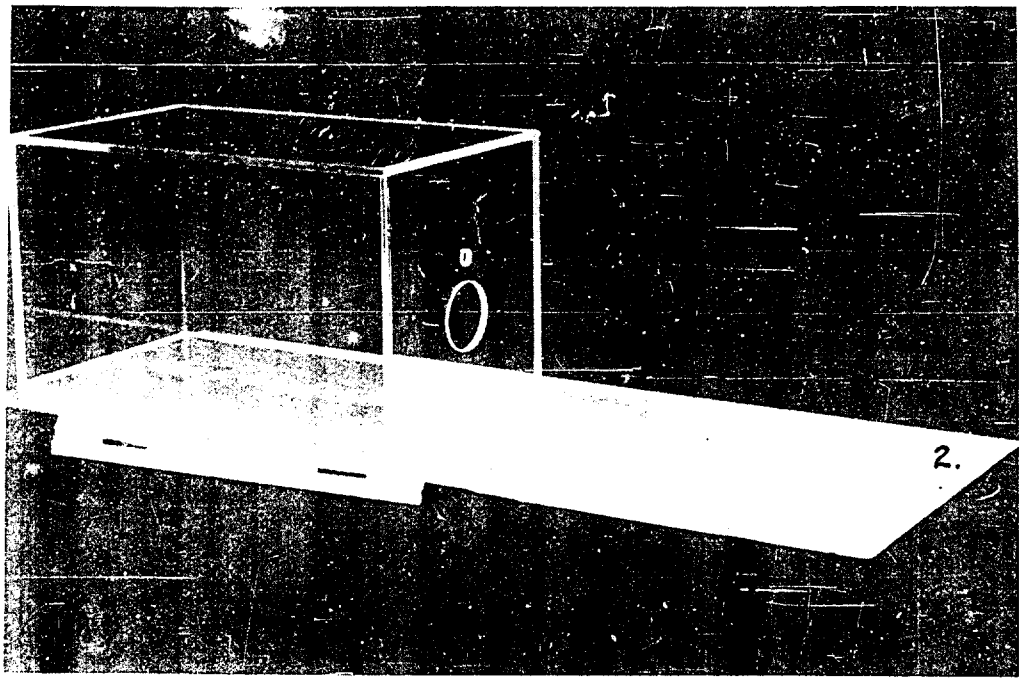

Figure 4.7

1. Plexiglass Container Mounted on EARC-I
2. Collection Plate

V. Theoretical Predictions

General

The variety of substances of which aerosols are composed and the wide range of particle sizes present in atomspheric air have made it necessary to use several methods simultaneously to investigate the size range of aerosols. Extensive data has been obtained with single instruments from which it is possible to show a coherent size distribution. Based upon such data, Junge has shown that particles in the range of 0.1 to 10 u radius have a size distribution which can be closely approximated by

$$\frac{dN}{d(\log r)} = \frac{\text{constant}}{r^B} \qquad (5.1)$$

where N = the total concentration of aerosol particles (per cm^3) from the lowest size limit to size r

B = a value between 2.5 and 3.5 depending upon geographic location and meteorological conditions. (Ref 5:9). Taken as 3.0 for theoretical calculations herein.

It is assumed for the purposes of this study that equation (5.1) does in fact represent the size distribution of natural aerosols. This assumption makes it possible to compare experimental data from EARC-I with similar theoretical calculations.

Computer Analysis

Stuart's computer solution of the charging equation (3.3) calculates the charge attained by a particle of given radius at any time, based upon the operating parameters of EARC-I. (Ref 13:12). With this base, a

program was written (Appendix A) and used to predict where each particle of a given group would be deposited by the precipitation process. Junge's distribution function provides the theoretical size distribution of particles which enter the precipitator.

Use is made of Fortran symbols in continuance of the style of Stuart, which makes following the computor program easier. Equation (5.1) is therefore re-written as

$$d(EN) = \frac{A}{RR^B} \cdot \frac{1}{RR} d(RR) \tag{5.2}$$

where EN = the density of aerosols (per cm^3) from the lowest size limit to the radius RR.

A = constant

B = same as in equation (5.1).

Letting a represent the lowest size limit,

$$\int_{EN_a}^{EN_{RR}} d(EN) = A \int_{a}^{RR} RR^{-B-1} d(RR) \tag{5.3}$$

and

$$EN(RR) - EN(a) = -A\left(\frac{1}{RR^B} - \frac{1}{A^B}\right) \tag{5.4}$$

where

RR = radius of particle of interest

EN(RR) = the total density per cm^3 of particles with radius a to particles with radius RR.

Fraction of Particles Collected (FRTO). Since the particle groups in this report include radii in a range of values, it is necessary to

derive an expression for the "density" of a given group. The density of particles in Group J is designated CONC(J), where J = 1, 2, ...9 and is called the concentration of group J. The concentration of particles in any group is found by subtracting the density from equation (5.4) using the smallest particle radius in that group, from the density, using the largest particle radius in that group, i.e.

$$\int_a^b f(x)\,dx = \int_m^b f(x)\,dx - \int_m^a f(x)\,dx \qquad (5.5)$$

As an example, consider particle Group 1 which includes particles with radii ranging from 1.0u to 2.0u. The concentration of particles of Group (1) is

$$CONC(1) = \left[EN\,(2) - EN\,(a)\right] - \left[EN\,(1) - EN\,(a)\right] \qquad (5.6)$$

which becomes from equation (5.4)

$$CONC(1) = -\frac{A}{B}\left[\frac{1}{a^B} - \frac{1}{RR(2)^B}\right] - \left(-\frac{A}{B}\right)\left[\frac{1}{a^B} - \frac{1}{RR(1)^B}\right]$$

and

$$CONC(1) = \frac{A}{B}\left[\frac{1}{RR(1)^B} - \frac{1}{RR(2)^B}\right] \qquad (5.7)$$

The general Fortran statement for any group J can be written

$$CONC(J) = \frac{A}{B}\left[\frac{1}{RR(J)^B} - \frac{1}{RR(J+1)^B}\right] \qquad (5.8)$$

where CONC(J) = the number of particles in group J (per cm^3).

To get the total number of group (J) particles which pass through EARC-I during a given sampling run, simply multiply the group concentration by the total volume of air sampled

$$CONC(J) \times V \qquad (5.9)$$

where V = total volume of air sampled (cm^3).

It follows that the total number of Group (J) particles collected at any point is equal to the total number which passed through the precipitator times the fraction of particles collected, FRTO

$$\text{FRTO}(J) \times \text{CONC}(J) \times V \tag{5.10}$$

where FRTO(J) = fraction of particles of group J collected. It is important to note how FRTO(J) was derived. The time is computed based on the particle's drift velocity. If the particle enters the precipitator this close or closer to the collection plate, it will be collected. If it is not within this distance, it will not be collected and will leave the precipitator with the airstream. (Ref 7:76).

Addition of the terms implied in equation (5.10) gives one the total number of all particles collected in groups 1 through 9

$$\sum_{J=1}^{9} \text{FRTO}(J) \times \text{CONC}(J) \times V \tag{5.11}$$

The fraction (of the total number of all particles collected from all nine groups) which is in any group J, is calculated by dividing equation (5.10) by equation (5.11):

$$\frac{\text{FRTO}(J) \times \text{CONC}(J) \times V}{\sum_{J=1}^{9} \text{FRTO}(J) \times \text{CONC}(J) \times V} \tag{5.12}$$

Equation (5.12) is the theoretical equivalent of the experimental data shown in Chapter VI. It is noted that the volume of air sampled, V, as well as the constant A/B from equation (5.7) cancel when calcula-

ting the final values to which the experiment data is compared.

Designation of Collection Points. There were a total of nine samples microscopically analyzed to gather the experimental data. To form a comparison for theoretical calculations, the following assumptions were made. Since each slide was traversed across the smaller dimension, i.e. 2.0 cm, a collection point was defined to be 2.0 cm wide as shown in Table 4.2. For the purpose of the computer program, the fraction collected at any given station, K, is the fraction collected at the upper limit of the station minus the fraction collection at the lower limit of the collection point.

For example, consider the fraction of particles in group 1, collected at station 5. From Table 4.2 one sees the collection point 5 extends from station 15.0 cm to 17.0 cm. Therefore for this example

FRTO(1,5) = FRTO(1, 17 cm) - FRTO(1, 15 cm).

The computer output is FRTO(J, K)

Where J = particle group number 1,2,3.....9

K = collection point number 1,2.3,....9

VI. Results

The results of the microscopic experimental investigation and the theoretical digital computer computations are shown in the graphs and tables which follow. A brief explanation precedes each group of data presented.

Experimental

The experimental data represent what was actually observed in the microscopic viewing of the samples collected at the nine collection points. Table 6-1 and Figures 6.1 through 6.9 show the number of particles in each group observed at the nine collection points. Table 6-2 is an expression of the same information in terms of the percent of the total sample considered at each collection point i.e. the 400 or more particles which were sized. For example, of the 446 particles sized at collection point 1, there were 317 which fell into group 1 (i.e. 317 particles had radii between 1.0 u and 2.0 u). That is 71.08% of the sample considered at collection point 1 were in group 1. Table 6-2 shows relative amounts for comparison with theory.

Qualitative Observations. During an experimental investigation there are certain observations made by the experimenter which are not amenable to a numerical classification. This situation results from such considerations as equipment limitations. As was mentioned previously, the theoretical limit of resolution for the optical microscope is approximately 0.2 u. Therefore attempts to measure particles in that size vicinity would result in highly questionable size distributions. Yet it is

Table 6-1

Number of Particles Experimentally Observed at Each Collection Point

Collection Point → / Particle Group ↓	1 0.1 to 2.1 (cm)	2 5.5 to 7.5 (cm)	3 8.0 to 10.0 (cm)	4 12.0 to 14.0 (cm)	5 15.0 to 17.0 (cm)	6 18.0 to 20.0 (cm)	7 21.5 to 23.5 (cm)	8 25.0 to 27.0 (cm)	9 30.5 to 32.5 (cm)
1	317	196	216	273	293	257	279	285	324
2	92	83	85	75	81	100	87	90	63
3	15	64	49	31	15	32	35	24	7
4	12	29	32	17	6	17	16	4	4
5	4	17	16	7	7	2	5	2	2
6	3	9	7	3	1	3	2	1	3
7	0	6	2	0	0	1	0	0	1
8	3	4	8	0	2	1	1	1	1
9	0	1	1	0	0	0	0	0	1
SAMPLE TOTAL	446	409	416	406	405	413	425	407	406

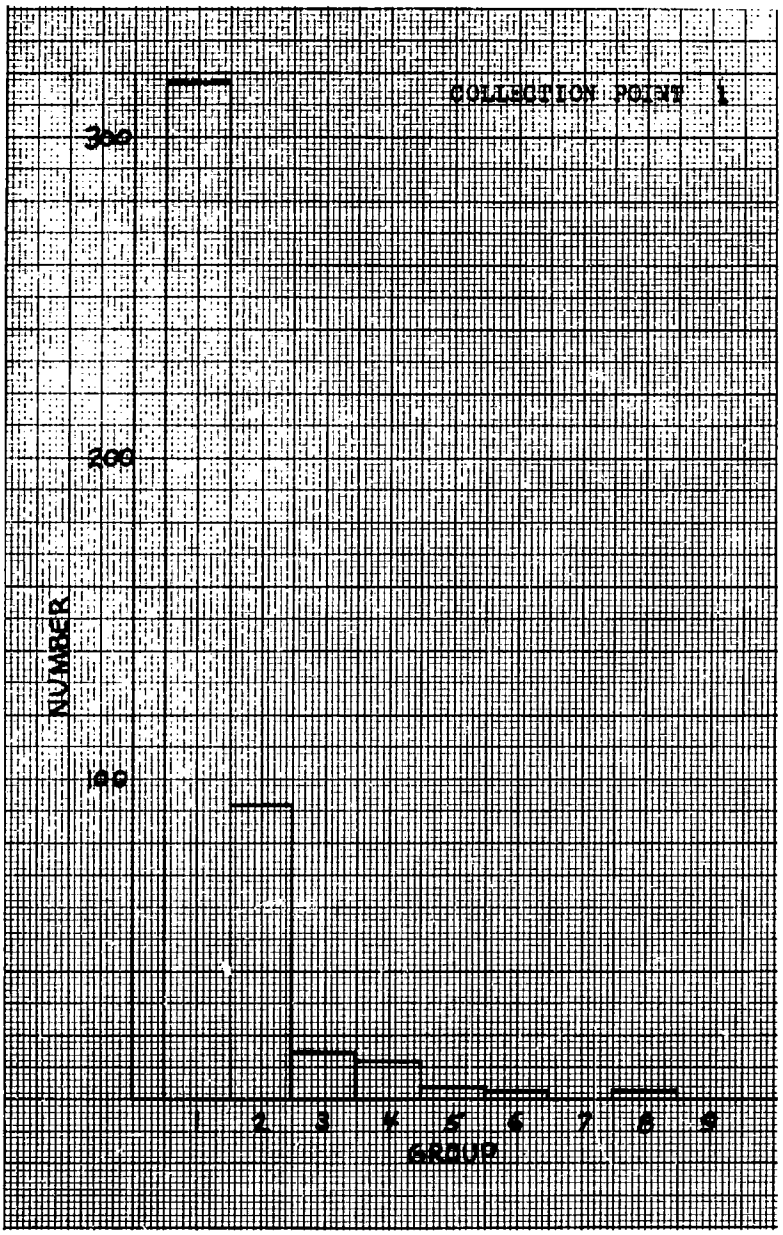

Figure 6.1

Number of Particles Experimentally
Observed in Each Group

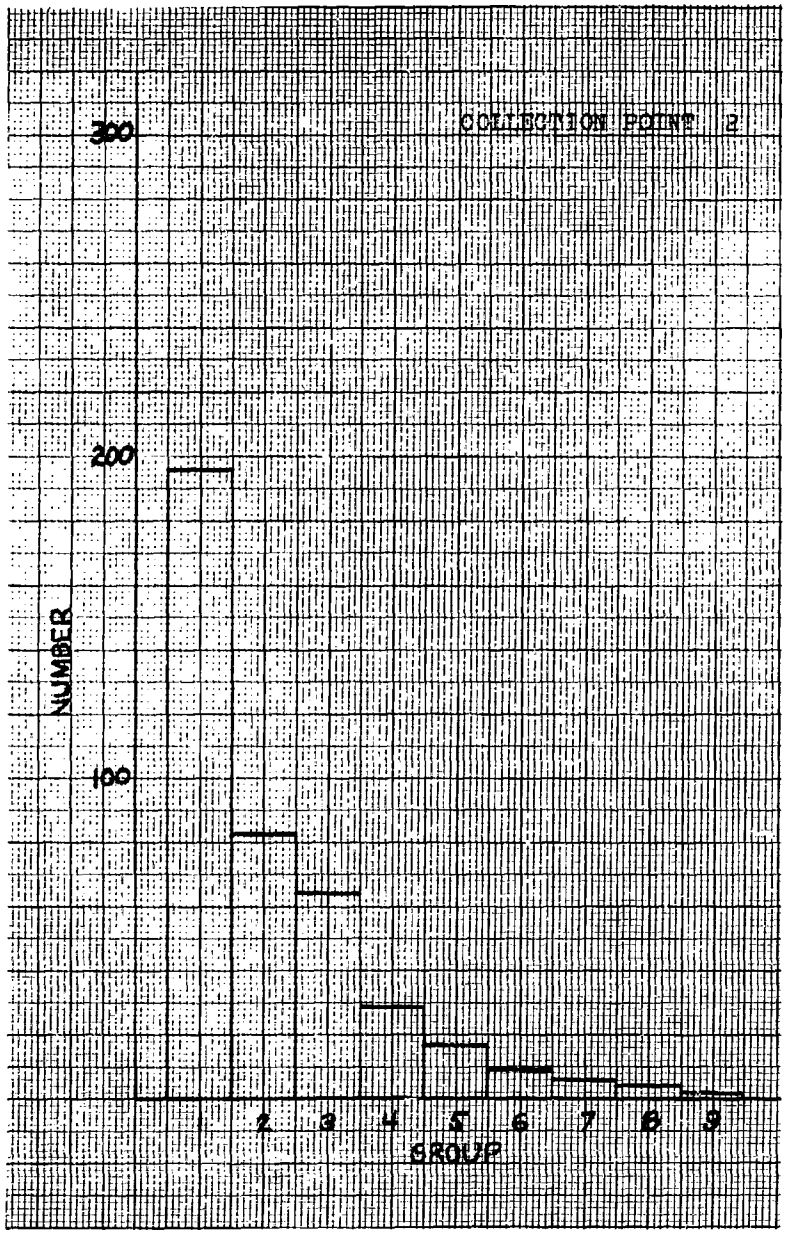

Figure 6.2

Number of Particles Experimentally Observed in Each Group

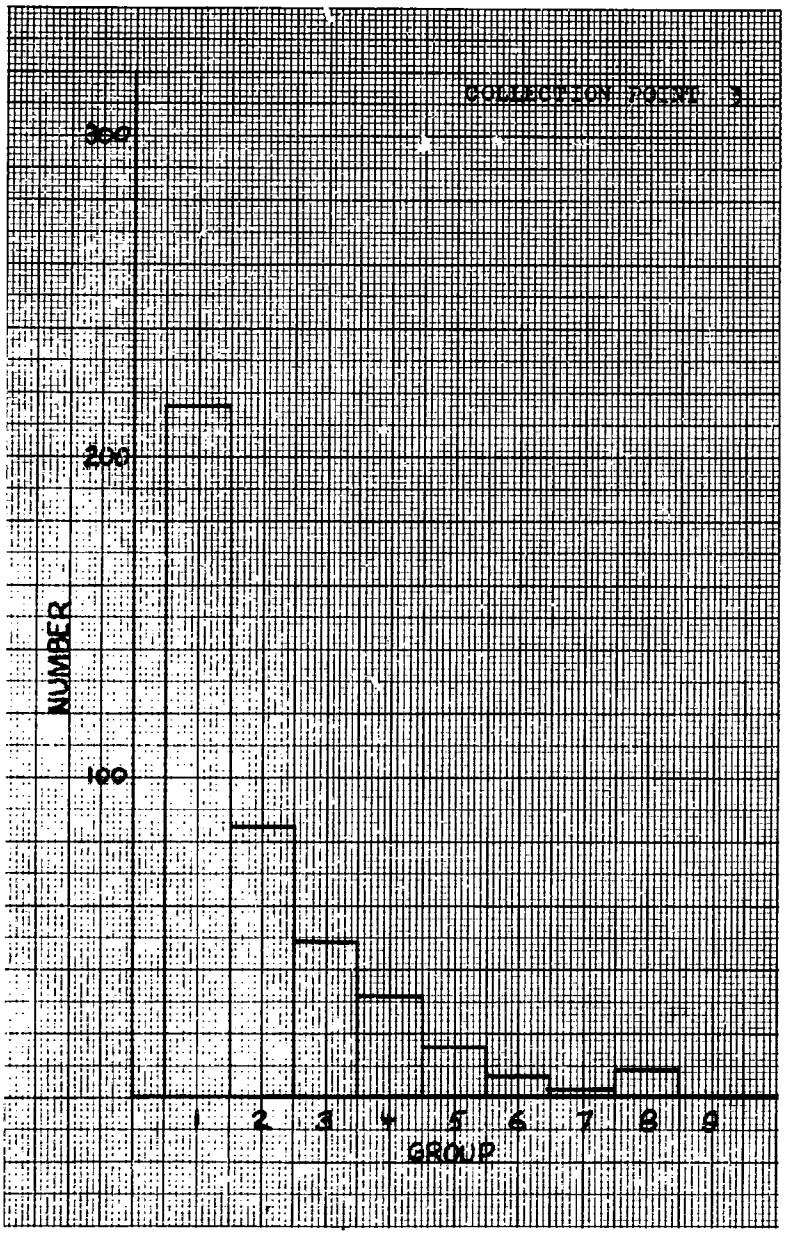

Figure 6.3

Number of Particles Experimentally Observed in Each Group

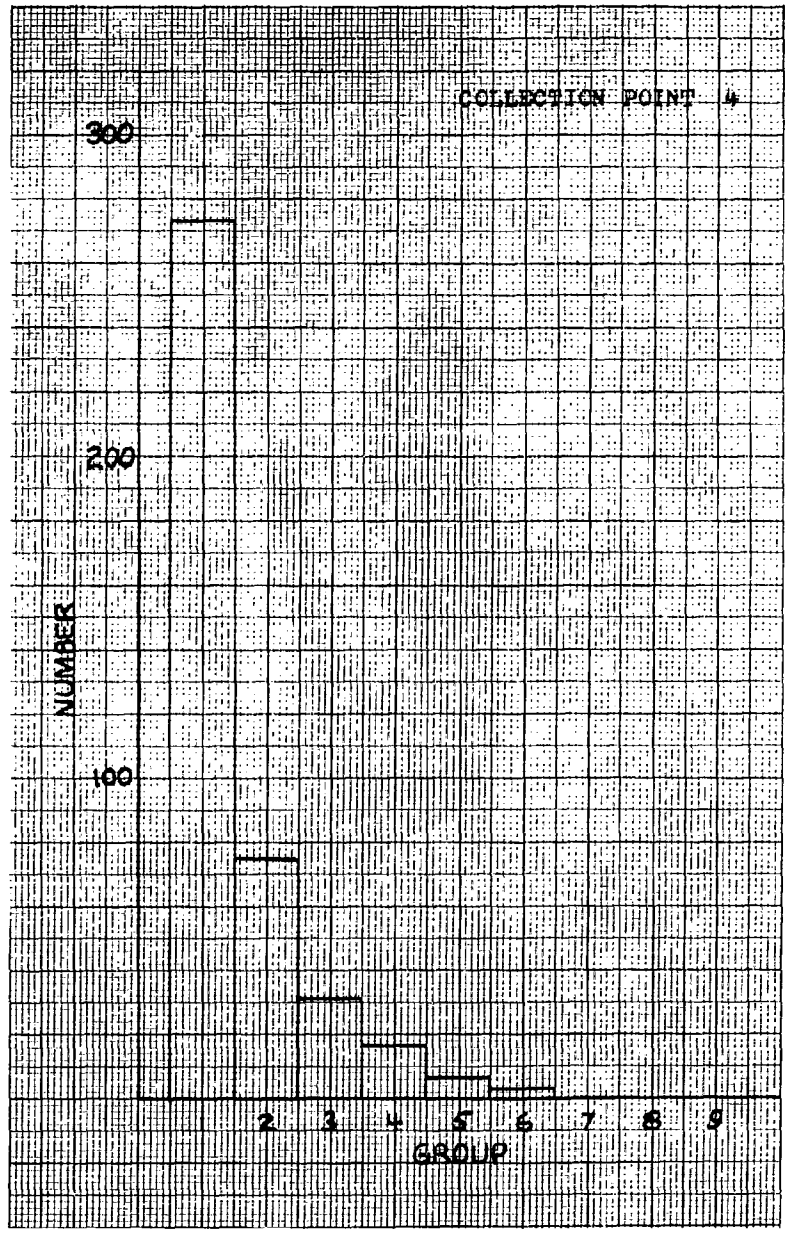

Figure 6.4

Number of Particles Experimentally Observed in Each Group

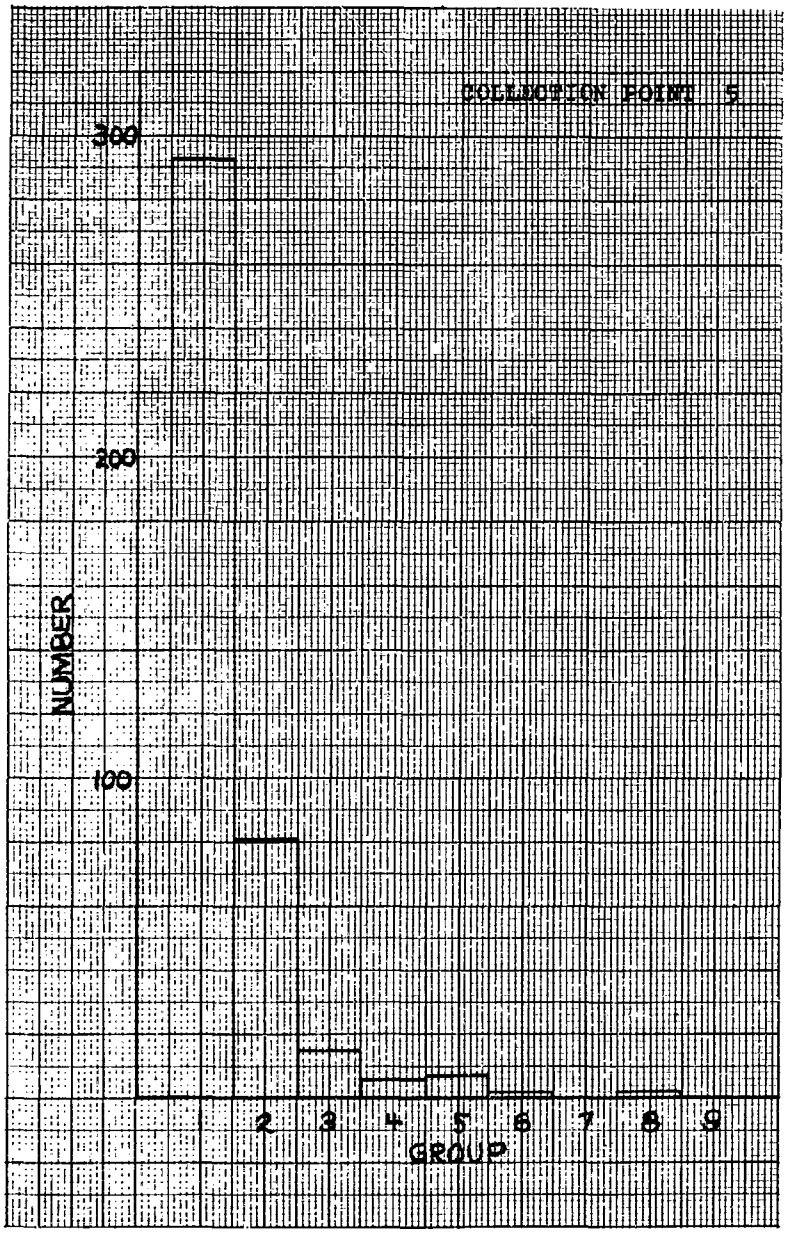

Figure 6.5

Number of Particles Experimentally
Observed in Each Group

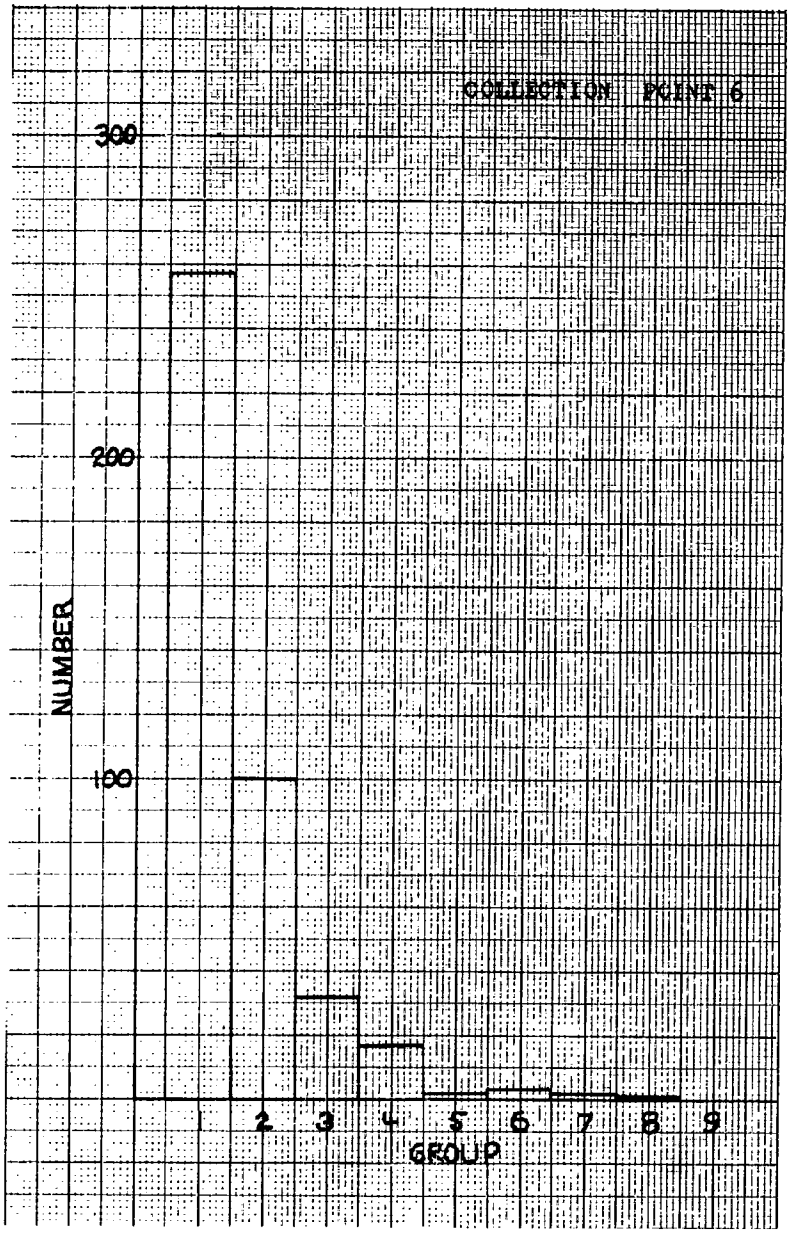

Figure 6.6

Number of Particles Experimentally Observed in Each Group

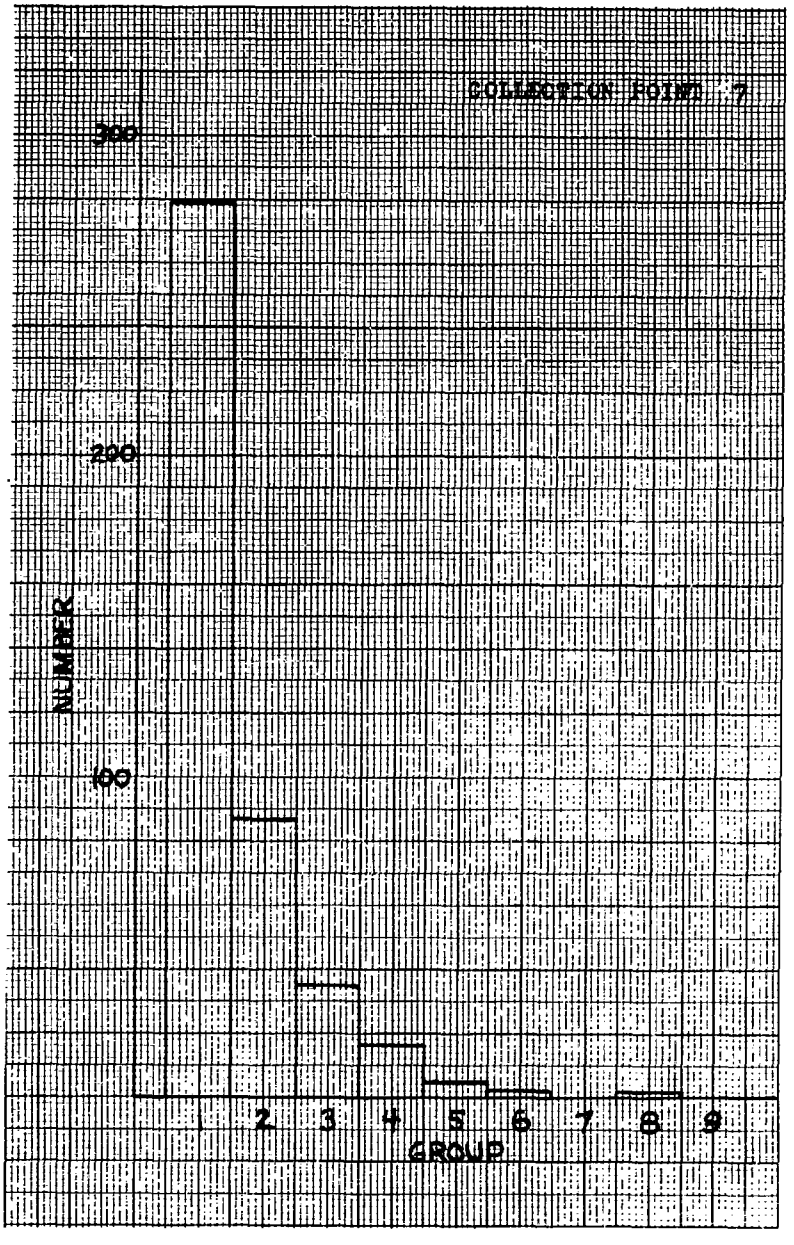

Figure 6.7

Number of Particles Experimentally
Observed in Each Group

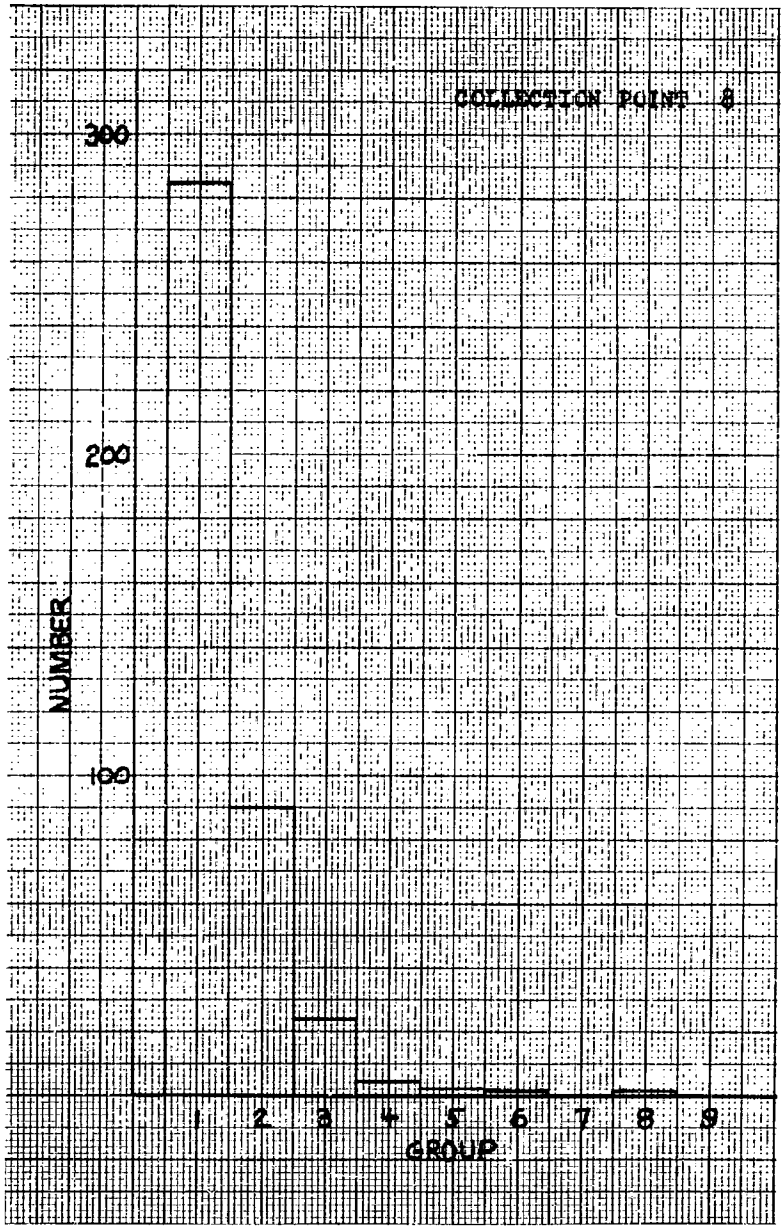

Figure 6.8

Number of Particles Experimentally Observed in Each Group

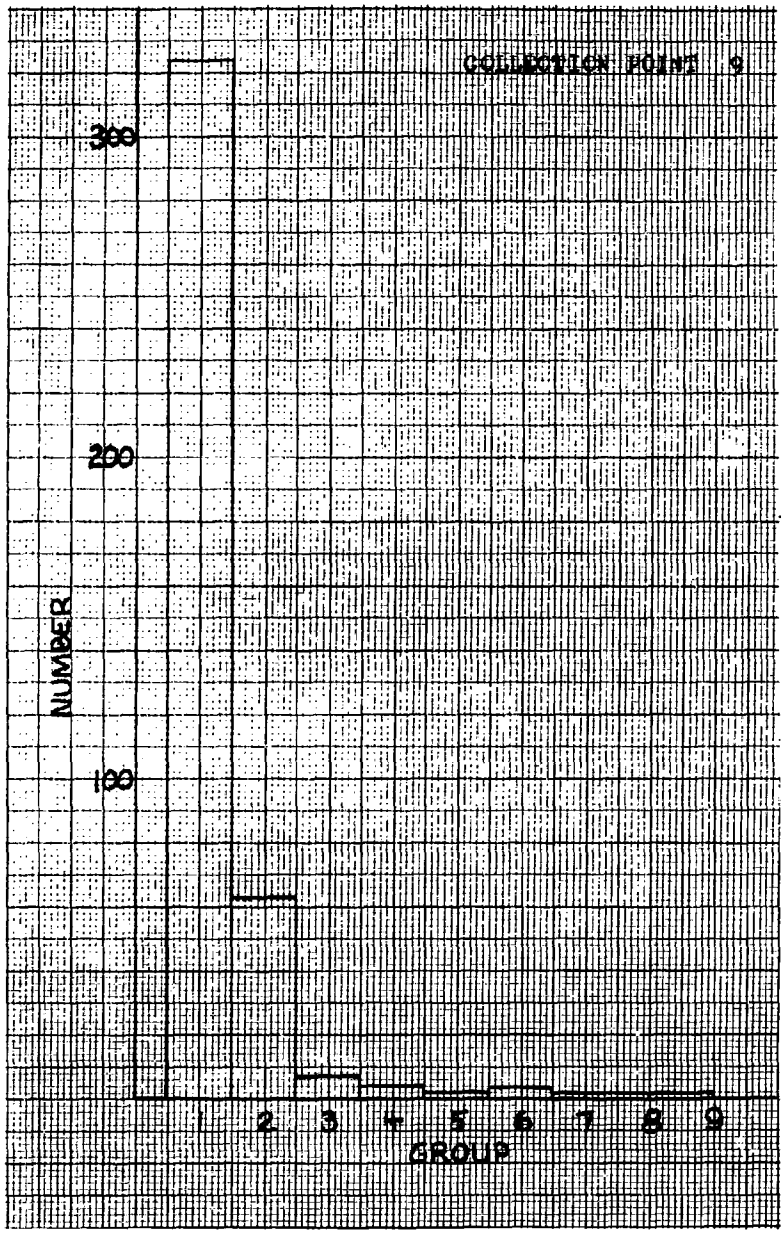

Figure 6.9

Number of Particles Experimentally
Observed in Each Group

Table 6-2

Percent of Total Sample Experimentally Observed from Each Group at Each Collection Point

Collection Point / Particle Group	1	2	3	4	5	6	7	8	9
1	71.08	47.92	51.92	67.24	72.34	62.23	65.65	70.02	79.80
2	20.63	20.29	20.43	18.47	20.00	24.21	20.47	22.11	15.52
3	3.36	15.65	11.78	7.63	3.70	7.75	8.23	5.90	1.72
4	2.69	7.09	7.69	4.18	1.48	4.12	3.76	0.98	0.98
5	0.90	4.16	3.85	1.72	1.72	0.48	1.18	0.49	0.49
6	0.67	1.45	1.68	0.73	0.25	0.73	0.47	0.24	0.74
7	0.00	0.98	0.48	0.00	0.00	0.24	0.00	0.00	0.25
8	0.67	1.95	1.92	0.00	0.49	0.24	0.23	0.24	0.25
9	0.00	0.24	0.24	0.00	0.00	0.00	0.00	0.00	0.25
APPROXIMATE TOTALS	100%	100%	100%	100%	100%	100%	100%	100%	100%

Example: At collection point 1, 71.08 percent of the particles sized were in particle group 1.

important to note that in general, the number of particles which this observer saw below 1.0 u in radius (i.e. the lower limit of the range of interest herein) far exceeds the number of larger particles recorded in Table 6-1. A conservative estimate would be to state that there were at least ten times as many particles with radii less than 1.0 u as there were particles counted in each group.

During the operation of EARC-I sparking was observed to occur in the collection section as well as the charging section. The sparking in the charging section was more pronounced than that in the collection section which is estimated to be at least a power of ten less frequent than sparking in the charging section. This observation has importance when considering the phenomenon of "back corona" which will be defined and discussed in Chapter VII.

Theoretical

The theoretical "data" presented here was arrived at by digital computation (see Appendix A for program listing). The theoretical equations developed by Lamberson for particle charging and fractions collected were manipulated to give an output which is the theoretical equivalent to experimental data presented in Table 6.2. This theoretical data is presented in Table 6.3. The operating parameters of EARC-I which were input for the computer program are listed below in Fortran symbols:

VL = 516.12 cm/sec	FRAR = 1023.75 cm^2
SEP = 2.00 cm	E = 9750 volts/cm
DL = 58.50 cm	CUR = 0.00125 amp
DCH = 12.7 cm	AREA = 331.47 cm^2
SEPC = 2.0 cm	ECOL = 7600. volts/cm

Table 6-3

Percent of Total Sample Theoretically Predicted from Each Group at Each Collection Point

Collection Point / Particle Group	1	2	3	4	5	6	7	8	9
1	78.50	79.79	81.84	89.19	100.	100.	0.	0.	0.
2	12.73	12.92	13.27	10.80	0.	0.	0.	0.	0.
3	4.27	4.34	4.45	0.	0.	0.	0.	0.	0.
4	1.94	1.97	0.42	0.	0.	0.	0.	0.	0.
5	1.04	0.83	0.	0.	0.	0.	0.	0.	0.
6	0.62	0.19	0.	0.	0.	0.	0.	0.	0.
7	0.40	0.	0.	0.	0.	0.	0.	0.	0.
8	0.27	0.	0.	0.	0.	0.	0.	0.	0.
9	0.19	0.	0.	0.	0.	0.	0.	0.	0.
TOTALS	100%	100%	100%	100%	100%	100%	0%	0%	0%

Example: Of the total particles collected at collection point 1, 78.50 percent of them should be in particle group 1.

Finally, for comparison purposes, a log-plot of the theoretical and experimental fractions of particles collected in each group at each collection point is presented in Figures 6.1 through 6.18.

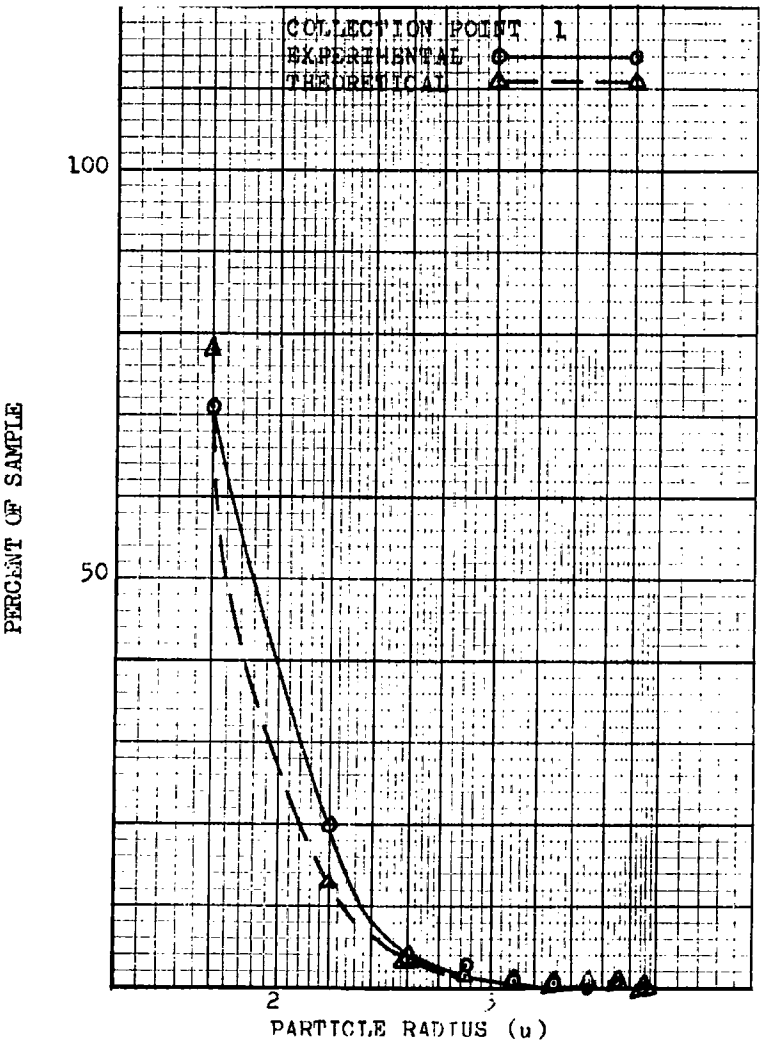

Figure 6.10

Experimental and Theoretical Percent of Sample vs Average Particle Radius

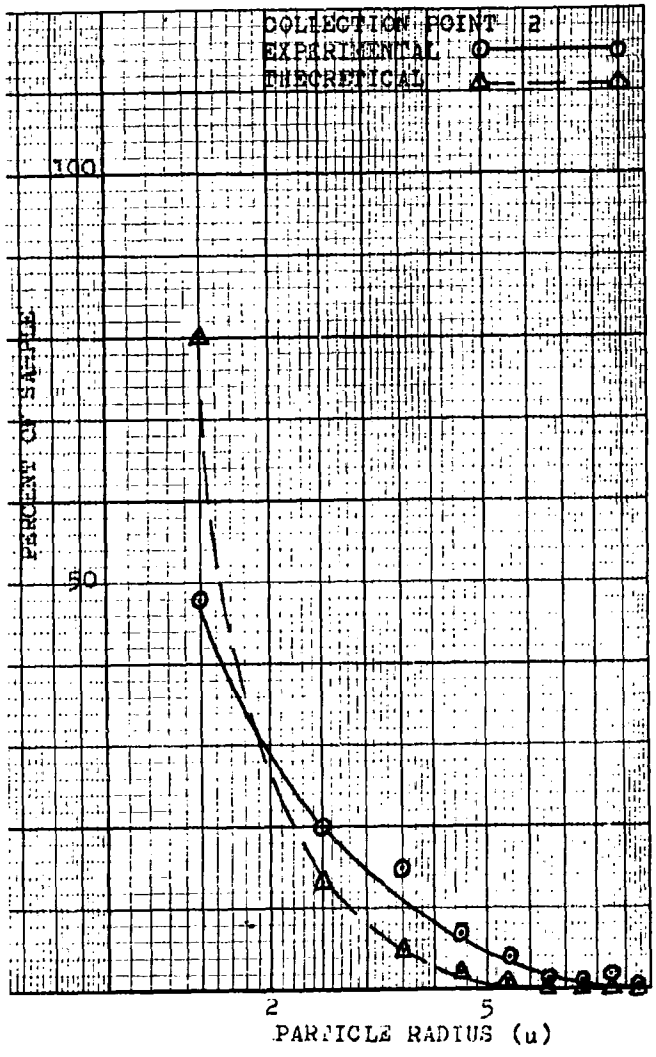

Figure 6.11

Experimental and Theoretical
Percent of Sample vs Average
Particle Radius

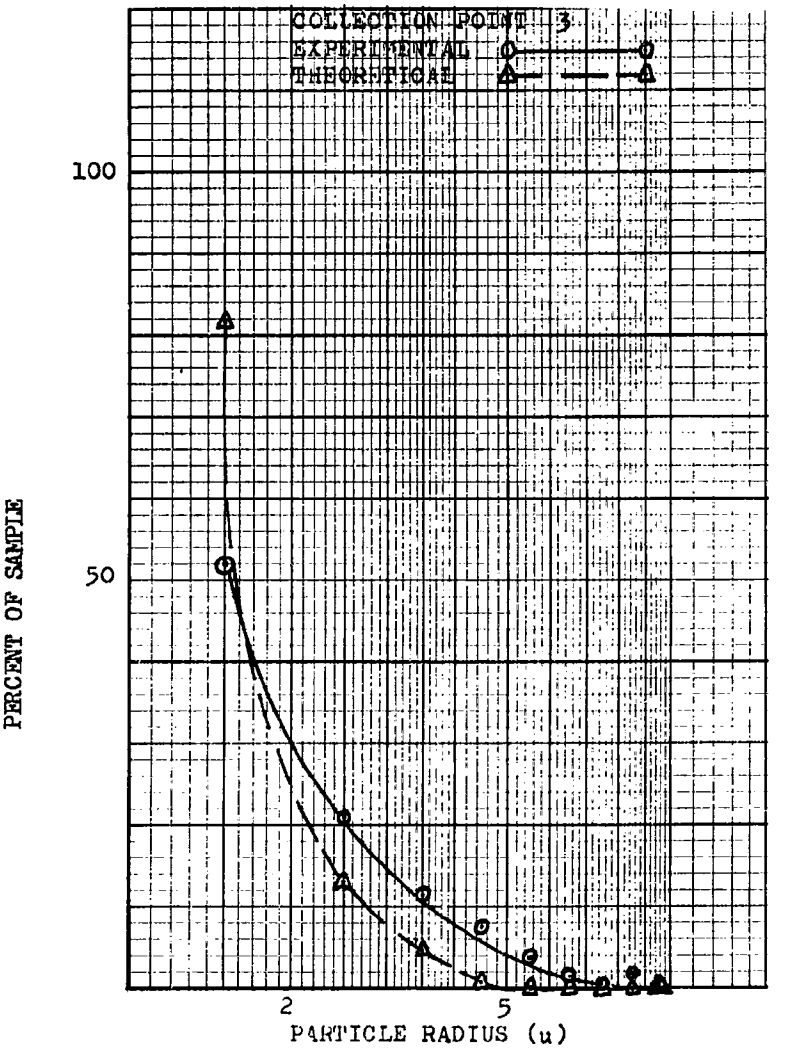

Figure 6.12

Experimental and Theoretical Percent of Sample vs Average Particle Radius

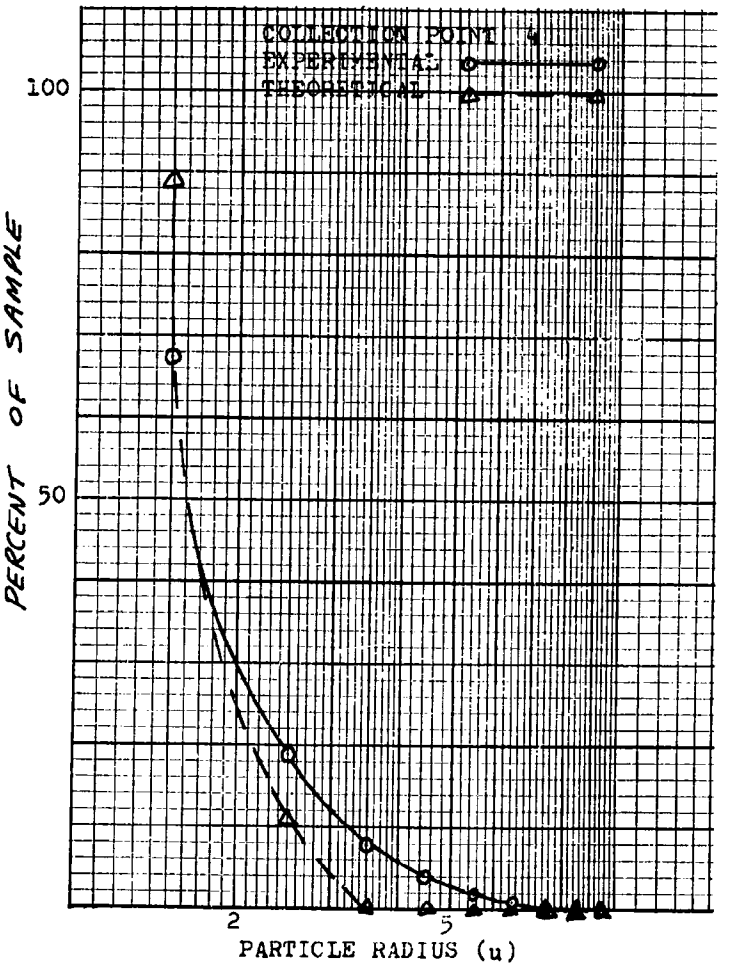

Figure 6.13

Experimental and Theoretical
Percent of Sample vs Average
Particle Radius

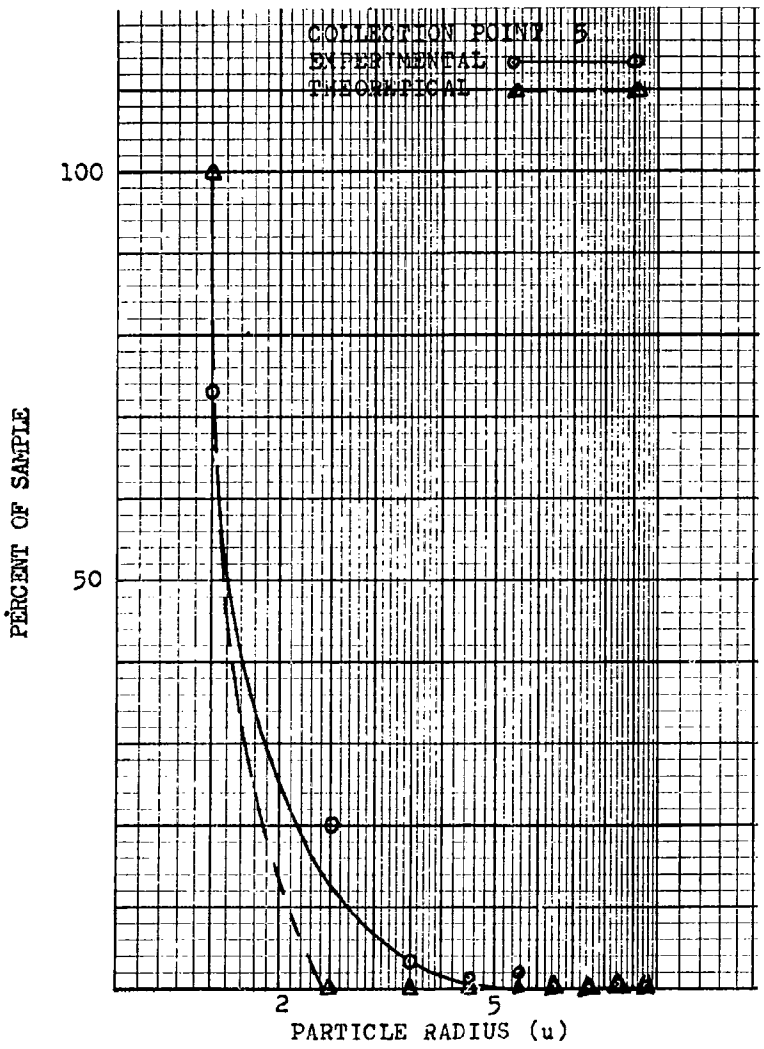

Figure 6.14

Experimental and Theoretical
Percent of Sample vs Average
Particle Radius

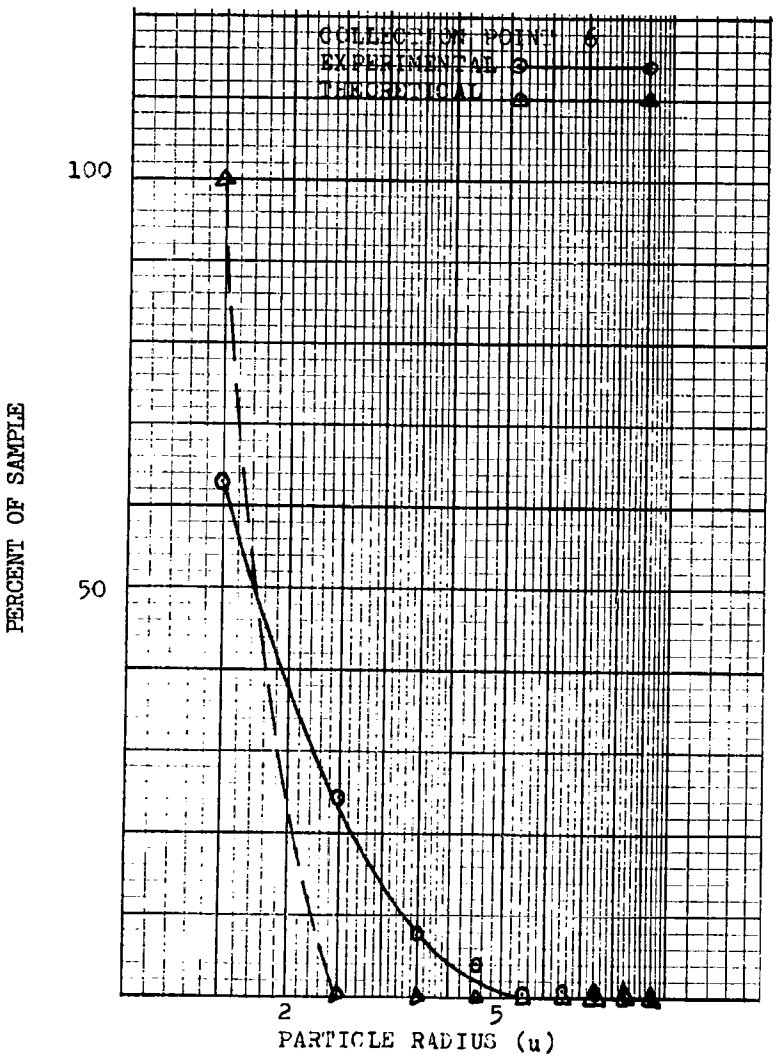

Figure 6.15

Experimental and Theoretical
Percent of Sample vs Average
Particle Radius

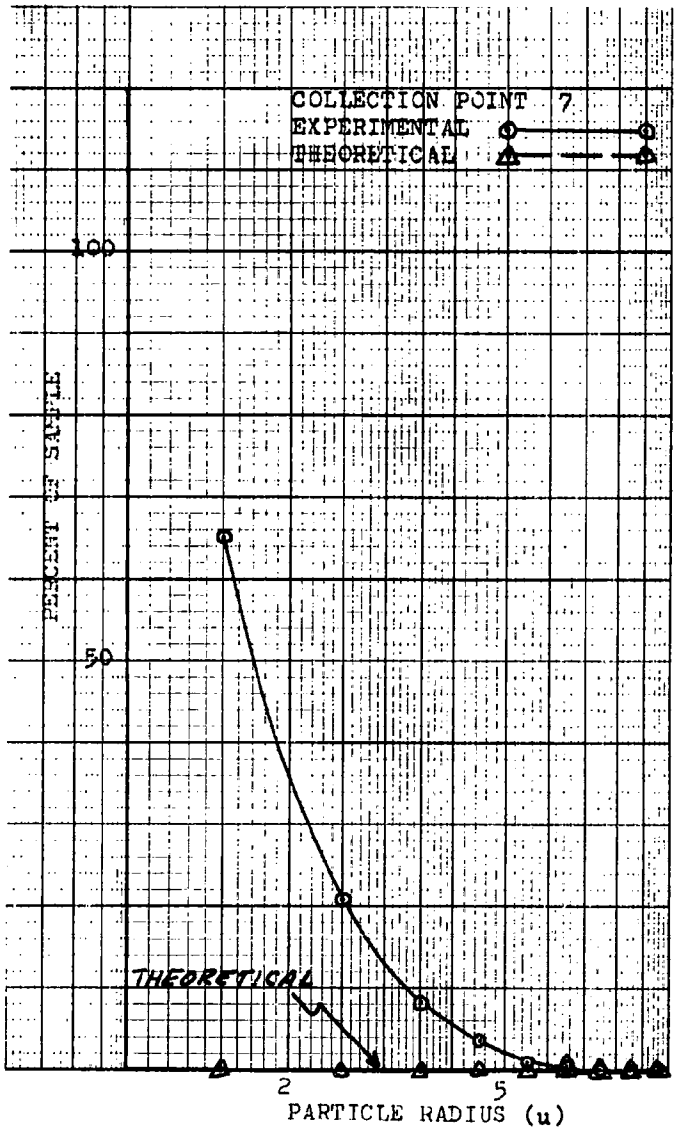

Figure 6.16

Experimental and Theoretical
Percent of Sample vs Average
Particle Radius

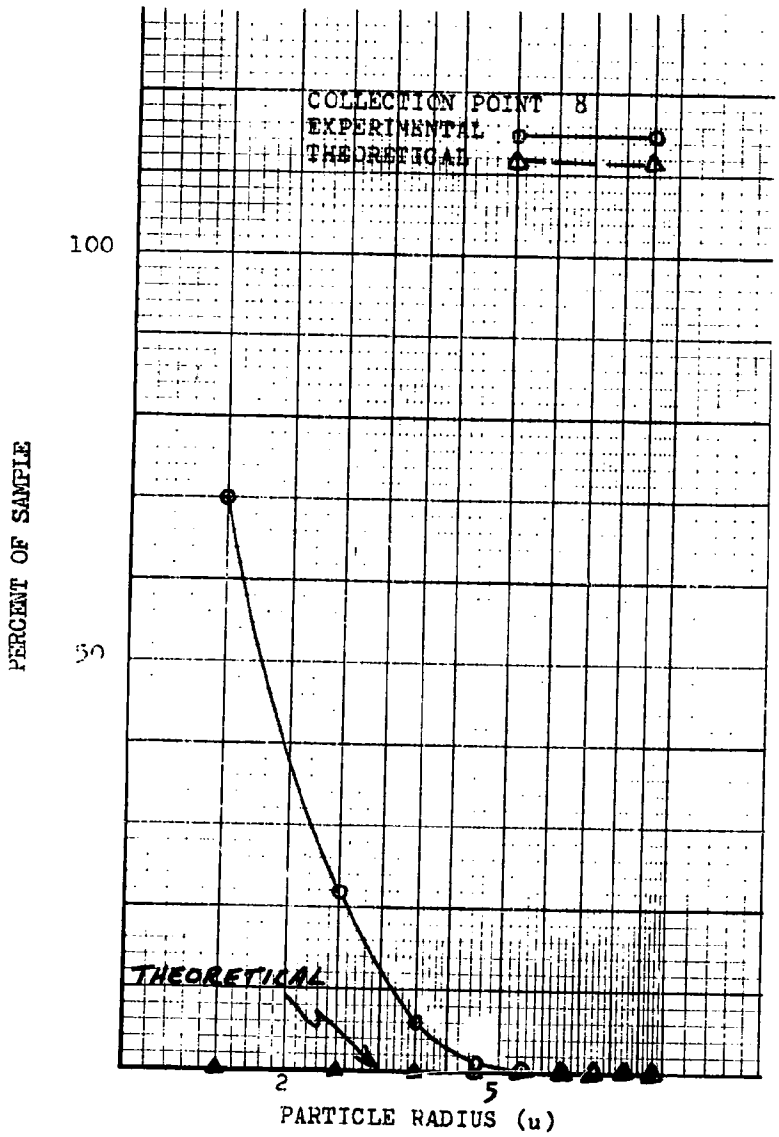

Figure 6.17

Experimental and Theoretical Percent of Sample vs Average Particle Radius

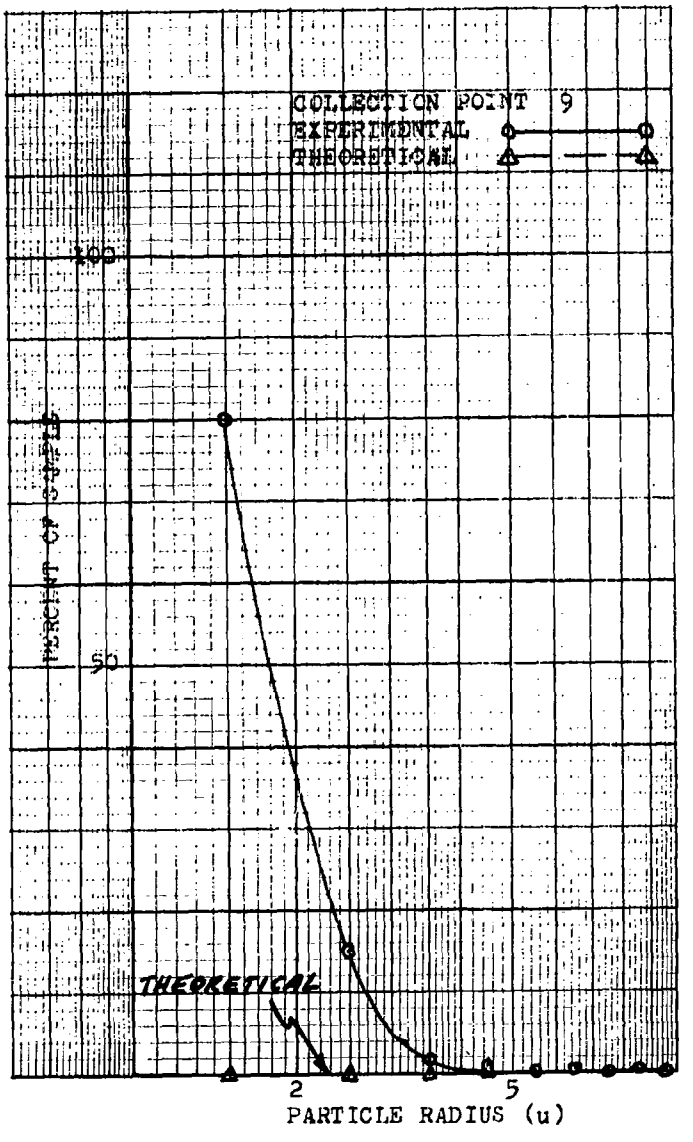

Figure 6.18

Experimental and Theoretical Percent of Sample vs Average Particle Radius

VII. Analysis and Conclusions

General

From an inspection of Tables 6-2, 6-3 and Figures 6.10 through 6.18 one can see that there are two extremes of agreement between the curves representing theoretical predictions and those representing experimental observations. On the one hand, there is exceptionally close agreement for collection points 1 through 5. That is, referring to the appropriate figures, one can see that for the first 5 collection points, the maximum deviation of experimental data from theory are as shown below:

Collection Point	% Deviation from Theory	Average Radius for Which Maximum Deviation Occurs
1	56.0	2.0
2	40.0	1.5
3	36.6	1.5
4	24.7	1.5
5	27.0	1.5

$$\text{where} \quad \%\ \text{Deviation from theory (for given radius} = \left| \frac{\text{theoretical \% of sample} - \text{experimental \% of sample}}{\text{theoretical \% of sample}} \right| \tag{7.1}$$

In general it can be seen that there is a larger deviation from theory for particles with smaller radii, for particles in the size range considered in this study.

On the other hand, beginning with collection point 6, there is an obviously increasing gap between the experimental and theoretical curves. At collection points 7, 8 and 9 there is an undefined deviation. Where theory predicts that no particles should be collected, microscopic analysis

shows that particles have been collected from all groups of interest. It must be noted, also, that the curves shown in Figure 6.10 through 6.18 are relative. They do not show a count of particles at the last collection point with reference to the first. That is, one cannot say from the experimental data collected, what percent of total number of particles which enter the precipitator, remain in the airstream by the time collection point 9 is reached. As an illustration, consider a test volume of air, containing N particles of all sizes, entering EARC-I. As that volume progresses downstream, particles are continually being removed by electrostatic precipitation. As the volume of air arrives at collection point 9, for instance, all that can be said about the test volume is that it contains less then the original N particles. It is quite possible then that at the later collection points the precipitation is working on a very small percent of the original number of aerosols which entered with the airstream.

Analysis of the results can be conveniently discussed in two parts. First there are the influences which occur from the time a given particle enters the precipitator until it is initially deposited. That is, until the time the particle first contacts the collection anode. Secondly there are phenomena which occur after a particle is deposited and which must be considered in relation to the experimental results observed.

Influences Prior to Initial Deposition

Dielectric Constant (K). In the equation (3.1) for bombardment charging, the dielectric constant, K, enters the expression in the factor

$$G = 1 + \frac{2(K-1)}{(K+2)} \qquad (7.2)$$

(Ref 7:35). Lamberson's calculated mean value of K = 4 by averaging materials usually found in urban areas is reasonable for arriving at a working value (Ref 7:21). However, for the specific case under consideration in this study, one must allow for K to vary between a value close to zero and very large values. In which case, G can be seen to vary between 0 and 3.

It can then be seen that the drift velocity of the particle is directly proportional to G, because from equation (3.1), saturation charge

$$q_o = G\, E,\, r^2 \tag{7.3}$$

The drag on the particle from Stoke's Law is

$$F = 6\pi r \eta V_o \tag{7.4}$$

and the electrostatic force between the particle and the collection anode is

$$F = q_o \epsilon E_2 \tag{7.5}$$

Equating the expressions for drag and electrostatic force, and substituting for q_o, the drift velocity (without Cunningham correction) is

$$v = \frac{G\, E_1\, E_2\, r}{6} \tag{7.6}$$

for a given set of precipitator parameters. It can be seen that two particles with the same radius, but with dielectric constants at opposite ends of their extreme values, could be deposited over a relatively wide range of collection points downstream of the entrance. At the extreme values of K, the relative collection point of the particle with the small K would be three times the distance to the collection point of the particle with the large K.

It is interesting to note further that as the particles with smaller radii are considered, the separation of collection points is more pronounced. This is evident by looking again to equation (7.6) and noting that the drift velocity is also directly proportional to the radius. A 1.0 u particle deposits farther downstream than a 10. u particle, for instance. This may explain in part the larger deviation between theory and experimental at the smaller radii.

Effects of the Field Distribution in the Charging Section. In the derivation of the equation for charging an aerosol by corona discharge, it was assumed that the electric field was a constant. The charging field is taken to be the value of the voltage potential between grid wire and anode, divided by their separation. This is really the expression for a linear field. A corona discharge is dependent, however, upon the field being non-linear. To derive an analytical expression for the field potential distribution in a corona field would be extremely difficult and has not been reported to date. Penney and Matick used a probe to measure the potentials in d.c. corona field for a plate to wire geometry. The experimental data thus obtained substantiates what one would intuitively expect the field to be. That is, the field would be greater at the wire and would decrease towards the plate. A characteristic plot of equipotential lines are shown in Figure 7.1.

It can be seen by inspection then that particles which enter the precipitator in any given plane parallel to the plate electrode will be under the influence of different values of electric field. In the extreme case, a particle entering the charging section along a wire electrode would see a field at least 1.5 times that of a field a particle which

entered in the same plane, but midway between two adjacent wire electrodes. The drift velocity would be greater than for particles closer to the corona wire. This effect was evident on the collection plates of EARC-I. On the charging section end of the plate, there was visible to the naked eye a layer of deposited dust forming an outline of the wire electrodes.

Field Distortion Between Charging and Collection Sections. Figure 7.2 shows a scale drawing of EARC-I with an exploded view of the physical point of separation between the charging and collection sections. Note that between the grid in the charging section and the negative plate in the collection section, there is a one-inch plexiglass insulator resulting in a one-inch gap between the grid frame and the negatively charged plate. The field distribution is conceptually indicated in the blowup of Figure 7.1. One can visualize the perturbation which a given particle "sees" compared to the orderly field present elsewhere. This perturbation most likely results in a contribution to the "spread" of points at station 5 and beyond (6,7,...).

Effects After Initial Deposition (Re-Entrainment)

The precipitator theory which has been developed here describes particle motion until it is initially deposited on the collection plate. However, one has no guarantee that a particle will not lose its charge on the collection plate and then be swept back into the airstream. Such particles might be deposited farther downstream or carried out of the precipitator with the exiting air. However, caused, the re-introduction of particles into the airstream is termed re-entrainment. It is important to note that a re-entrained particle is not necessarily lost, since it can be redeposited downstream of its initial point of deposit. Baker (Ref 1:40) used a Gelman

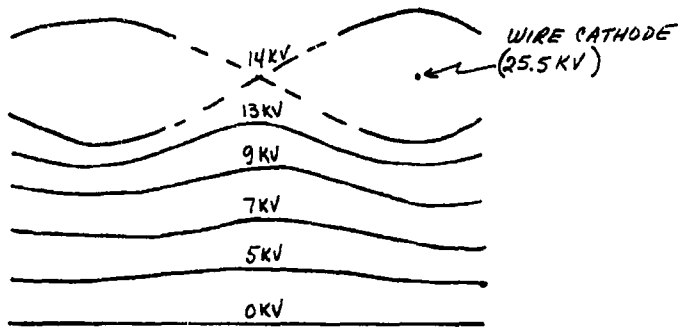

Figure 7.1

Typical Equipotential Lines in
Plane-to-Wire Geometry (Ref 10:95)

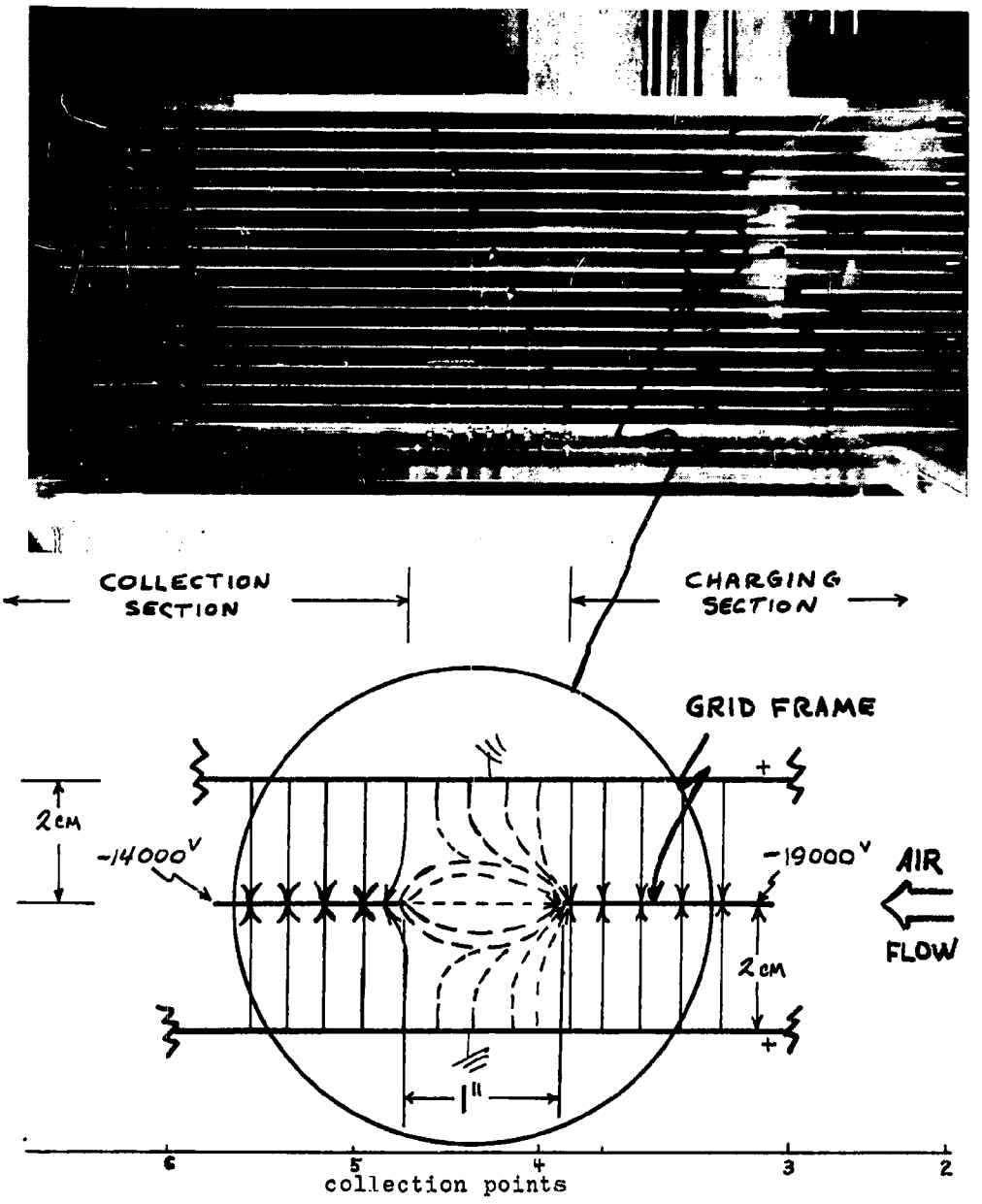

Figure 7.2

Side View of EARC-I with Full-Scale Exploded View of Air Gap between Grid and Negatively Charged Plate and True Locations of Collection Points 2 - 6.

Air Sampler to examine air immediately as it left EARC-I. He found negligible dust traces on a 2.0 micron Gelman filter paper, following 4-hour sampling runs. This would indicate that re-entrainment for 2-micron and larger is negligible in the sense that such particles escape from EARC-I. However, the possibility exists that "internal" re-entrainment followed by re-deposition could occur in EARC-I. Such a phenomenon could also cause particles to be observed where theory would preclude their collection. This is especially pertinent to larger particles since they should plate out before smaller particles in the range considered in this study. Re-entrainment may explain the larger particles experimentally observed at collection points 7, 8 and 9.

Formation of a Layer of Collected Particles. As a means of determining the efficiency of a precipitator, Lamberson derived an expression for the fraction of particles which would be collected for any given group, FRTO (Ref 7:73). This fraction is based on the simple geometric relation between the distance the particle travels towards the collection plate while it is in the precipitator, and the total interelectrode distance:

$$FRTO = \frac{\text{distance particle travels towards collector electrode during the time it spends in precipitator}}{\text{distance between electrodes}} \qquad (7.7)$$

Considering equation (7.7) in relation to identical particles which enter the precipitator at the same distance from the collection plate, it must be concluded that theoretically each such particle will be deposited at the same point downstream of the entrance. The result would be an eventual "pile-up" of the identical particles hypothetically considered here. Such a situation in EARC-I, where the plates are used dry (not treated with an

adhesive to retain deposited particles) could result in erosion, by the airstream, of the particles at the surface of the collected layer. For particles re-entrained in the charging section, there is the likelihood that they would be immediately recharged and redeposited. For particles re-entrained in the collection section, where there is no corona, recharging is not possible. The particle may then leave the precipitator with the effluent airstream or be redeposited if it has retained a residual charge. The above possibility is in essence a case of re-entrainment caused by physical limitations of the equipment. That is, the collection and retention of an unlimited number of aerosols at a given point is not a logically acceptable tenet.

Back Corona. Another cause of re-entrainment is the phenomenon known as back corona or reverse-ionization. A particle which has been deposited on the clean collector anode will give up its negative charge and assume the polarity of the collector. The result is a repulsive force. The particle will be repulsed if the Coulombic repulsion is greater than the molecular forces of attraction which exist between the particle and collector. For very small particles, molecular forces predominate and retain the collected particles (Ref 8:540). This effect was noted by Baker (Ref 1:44) who struggled with the problem of removing deposited particles from the collection plate of EARC-I, in order to concentrate them into a sample which could be used for radioactivity analysis. He was successful only after resorting to ultrasonic cleaning. Order of magnitude calculations by Lowe (Ref 8:547) indicate that larger particles with high conductivity will be repulsed from the collector. If a previously deposited

layer of particles covers the anode, a voltage potential will develop across the layer for resistivities greater than 10^{10} ohm-centimeters. Local breakdown occurs (back corona) creating ions of polarity opposite to the cathode, thus neutralizing the original action of the precipitator. Since the entrance to EARC-I is fitted with a wire screen to keep out extremely large pieces of airborne debris, the back corona is a logical explanation for the sparking which occurs during the normal operation of EARC-I.

Summary of Analysis

It is evident from the topics discussed above that there are many phenomena which can enter into the total process of electrostatic precipitation. The factors listed above are listed as possible explanations for the deviations between theoretical and experimental data. They are offered as possible explanations only because an investigation of the phenomena themselves was not an object of this study. It is an indication of the imperfection of the model introduced by Lamberson (Ref 7) that such phenomena cannot be treated in an analytically rigorous manner. However, in spite of these phenomena, Lamberson's simple model does give some correlation as shown in Figure 6.10 through 6.18.

Conclusions

The experimentally determined size distributions of precipitated aerosols at the various collection points when compared to the expected size distribution at the same collection points lead one to conclude that EARC-I does collect particles roughly in accordance with Lamberson's model. The assumptions made in the original derivation of the theoretical

model plus the variable quantities inherent in atmospheric aerosols not only explain, but indeed lead one to expect the deviations observed in the two sets of data.

The two basic assumptions are here restated in view of the possible conclusions to be drawn. That is, the theoretical and experimental data should agree reasonably well; if the size distribution of naturally occuring aerosols is that described by Junge and if EARC-I does operate as described by Lamberson's model. These assumptions are reiterated to mention that the remote possibility exists that both assumptions may be wrong and that the errors in one cancel the errors in the other. This possibility is considered to be unlikely.

VIII. Recommendations

In spite of the lack of a complete understanding of electrostatic precipitators, their use has increased since the early 1900's. Industry has used them effectively for the use of relatively large particulate matter such as fly ash from power stations. Baker has demonstrated conclusively that EARC-I in its present form does collect more than adequate amounts of particulate matter for analyzing the atmosphere for its radioactivity content. This is true although the method he used for secondary concentration of collected samples of airborne particulates most probably involved much loss of the originally precipitated matter.

The literature reviewed by this author during the course of this investigation leads him to conclude that the theory has not changed substantially since the first electrostatic precipitators. On the other hand ingenious engineering has rendered them useful in a wide variety of situations, in fact, even where theory would preclude their use (Ref 11:97). It is therefore recommended that the development of EARC-I be continued from an engineering-development point of view rather than to pursue further theoretical analyses.

Observations made during the microscopic phase of this study confirm the thought that electrostatic precipitators are especially efficient in the precipitation of small particles. However, for the purpose of radioactivity detection, one cannot consider a particle properly precipitated until it has been removed from the atmosphere and conveniently placed under a detector for analysis. Therefore, for future Air Force and/or Civil Defense use, engineering sophistication of EARC-I should be effected

in the following specific areas, listed in the order of their importance:

1. Find or devise an easily removable and compressible coating which can be applied to the collection plates of EARC-I. The requirement for compressibility is intended to include any means of making a collected sample small enough to be used with existing radiation detectors.

2. Find or devise a method of making the coating highly conductive and adhesive in order to render the coating electrically identical to the collection plate. This would lead towards 100% retention of deposited particles because of the combined effects of the Coulombic attraction and adhesive quality.

3. Investigate the effects of reducing the collection plate area. The ultimate aim is to attain a small one-stage precipitator.

4. Redesign EARC-I to facilitate the removal and installation of the plates and grids.

If it is desired to continue investigating the manner in which EARC-I collects microscopic particles, one could use a radioactivity tracer method in the following general manner:

1. Introduce particles* of known size and material (hence constant K) impregnated with a known radioactivity into the inlet airstream.

2. Measure the level of radioactivity at various points along the collection plate.

* Physical Research Laboratory, 280 Building, Dow Chemical Company, Midland, Michigan has available Polystyrene spheres which come in the following sizes: 0.09 u, 0.19 u, 0.26 u, 0.37 u, 0.56 u, 0.81 u, 1.1 u and 3.0 u. It also has the following size mixtures available: 6.0-14.0u, 16.0-28.0 u, 29.0-56.0 u, and 49.0-105.0 u. Such a spectrum of sizes would allow for a wide range of investigation.

3. Calculate the number of particles required to give the level of activity detected at each test point.

4. Repeat the procedure on clean plates using particles of the same material as in 1 but with a different known radius.

The procedure suggested above would correct the limitations inherent in sampling naturally occuring aerosols as was done in this investigation. Specifically, one could:

1. Know the absolute number of particles introduced into the precipitator.

2. Know the dielectric constant, K

3. More closely approach the assumption that all particles are spherical.

A tracer technique would also lend itself to investigating re-entrainment. Re-entrainment could be studied, for example, by pulsing the radioactive particles into the entrance and observing the radiation response as a function of both distance and time after pulse.

Bibliography

1. Baker, J. W. Sampling of Airborne Radioactive Particles by Electrostatic Precipitation. M.S. Thesis, Air Force Institute of Technology, 1962.

2. DallaValle, J.M. Micromeritics (Second Edition). New York: Pitman Publishing Corporation, 1948.

3. Herdan, G. Small Particle Statistics (Second Edition). New York: Academic Press Inc., 1960.

4. Hewitt, G. W. "The Charging of Small Particles for Electrostatic Precipitation." Transaction: American Institute of Electrical Engines, Communications and Electronics - Part I, 76: 300-306

5. Junge, C. E. "Atmospheric Chemistry." Advances in Geophysics, 4 New York: Academic Press Inc., 1958.

6. Junge, C. E. "The Chemical Composition of Atmospheric Aerosols I: Measurements at Round Hill Field Station, June-July 1953." Journal of Meteorology, 11: 323-333 (August 1954).

7. Lamberson, D. L. A Study of the Electrostatic Precipitation of Radioactive Aerosols. M. S. Thesis, Air Force Institute of Technology, 1961.

8. Lowe, H. J. and Lucas, D. H. "The Physics of Electrostatic Precipitation." British Journal of Applied Physics, Supplement 2: S40 - S47 (1953).

9. Murphy, H. T. et al. "A Theoretical Analysis of the Effects of an Electric Field on the Charging of Fine Particles." Transactions: American Institute of Electrical Engineers, Communications and Electronics - Part I, 78: 318 - 325 (September 1959).

10. Penney, G.W., and Matick, R. E. "Potentials in D-C Corona Fields." Transactions: American Institute of Electrical Engineers, Part I, 79: 91-99 (May 1960).

11. Rose, H.E., and Wood, A.J. An Introduction to Electrostatic Precipitation in Theory and Practice. London: Constable and Company Ltd., 1956.

12. Skinner, D.G., et al. Determination of Particle Size in Sub-Sieve Range. London: The British Colliery Owners Research Association, 1944

13. Stuart, R.S. The Analysis, Optimization, and Design of an Airborne Radiation Sampling Electrostatic Precipitator. M. S. Thesis, Air Force Institute of Technology, 1962.

14. White, H.J. "Modern Electric Precipitation." Industrial and Engineering Chemistry 47: 932-939 (May 1955).

15. White, H.J. and Penney, G.W. "Electrical Precipitation Fundamentals." Engineering Proceedings P-39 (July 1961).

16. White, H.J. "Particle Charging in Electrostatic Precipitation." Transactions: American Institute of Electrical Engineers - Part II, 70: 1186-1191 (1951).

17. No Author. Photomicrography with the Vicker Projection Microscope. York, England: Cooke, Troughton, & Simms.

18. No Author. "Reference Manual for the Southern Research Institute Particle Size Analyzer" Birmingham.

Appendix A

Fortran Program Used for Theoretical Computations

General

The IBM 7090 Digital Computer was used to solve the theoretical equation describing the motion of particles as they flow through EARC-I. A description and listing of the Fortran program used follows. The dictionary of variables is listed elsewhere because the text of this report uses Fortran symbols where possible to facilitate understanding the program. Since this is a modified version of Stuart's program (Ref 13) which is explained thoroughly in his thesis, only a brief program description is offered below.

Program Description

The purpose of this program is to compute the fraction of particles in each group collected at each collection point based upon the theoretical equations described in previous chapters. The program also has the convenience of computing experimental fractions so collected, based upon the input of experimental data.

The basis of the program is found in statements number 691+1 through statement number 35. This section of the program computes the total charge a particle has attained at any time from t = 0 seconds to t = 1001 seconds at 0.0001 - second intervals. From the charge QQ the drift velocity of the particles of interest is computed for any time; and as described in the text, the point at which the particle is finally theoretically deposited. Statements number 799 through 804 accomplish the latter computations. The program is then cycled nine times, once

for each particle group then eight times on top of that. The latter eight cycles are arbitrary. They are for the purpose of observing the effects by varying the exponent BETA of Junge's differential equation for aerosol distribution in the atmosphere.

The output of the program is a listing of the theoretical prediction of the fraction of each particle group collected at each collection point for each value of BETA investigated. The output is in the form of an array the rows representing particle groups 1 through 9; the columns representing collection points 1 through 9. All output is labeled with an appropriate heading.

Fortran Program Listing

BEST AVAILABLE COPY


```
10   COMPUTATION OF FRTO(J,K) USING AVERAGE RADII(1.5, 2.5....9.5)

     DIMENSION Q(1001),R(9),CUN(9),V(1001),CONC(9)
     DIMENSION TSTN(18),STN(18),FRTO(9,18),COLM(9),EN(10),RR(10)
     DIMENSION FR(9),FRC(9,9),SEN(9),EFF(9)
     DIMENSION EXPER(9,9),EXCOL(9),XFRTO(9,9)
 100 FORMAT(E11.4)
 115 FORMAT(5X,33HFRACTIONS COLLECTED - THEORETICAL,//(9E14.6/))
 120 FORMAT(5X,7HBETA = E14.8/)
 130 FORMAT(5X,36HFRACTIONS COLLECTED - EXPERIMENTALLY,//(9E14.6/))
 131 FORMAT(5X,6HCUN(J),//(9E14.6/))
 132 FORMAT(5X,48HNUMBER OF PARTICLES IN EACH GROUP - EXPERIMENTAL,//(9
    1E14.6/))
 133 FORMAT(5X,24HMASS FRACTIONS PER GROUP,//(9E14.6/))
   2 READ INPUT TAPE 2,100,(R(J),J=1,9)
   3 READ INPUT TAPE 2,100,VL,SEP,DL,DCH,SEPC,FRAR,E,CUR,AREA,ECOL
 500 READ INPUT TAPE 2,100,(STN(K),K=1,18),(RR(K),K=1,10)
     READ INPUT TAPE 2,100,((EXPER(J,K),J=1,9),K=1,9)
5000 DO 5001 J=1,9
5001 CUN(J)=1.+((9.42E-6)*((1.23)+(.4)*EXPF((-0.734)*(10.**(5.*R(J)))))
    1))/(R(J))
     DO 5002 K=1,9
     EXCOL(K)=0.
     DO 5002 J=1,9
5002 EXCOL(K)=EXCOL(K)+EXPER(J,K)
     DO 5003 J=1,9
     DO 5003 K=1,9
5003 XFRTO(J,K)=EXPER(J,K)/EXCOL(K)
     DO 5005 J=1,9
5005 FR(J)=LOGF(RR(J+1)/RR(J))
     WRITE OUTPUT TAPE 3,131,(CUN(J),J=1,9)
     WRITE OUTPUT TAPE 3,132,((EXPER(J,K),K=1,9),J=1,9)
     WRITE OUTPUT TAPE 3,133,(FR(J),J=1,9)
     BETA=1.
     DO 2000 N=1,8
     WRITE OUTPUT TAPE 3,120,BETA
     DO 69 K=1,10,1
  69 EN(K)=1./RR(K)**BETA
     DO 691 J=1,9
 691 CONC(J)=EN(J)-EN(J+1)
     J=1
     DELT=0.0001
     VLCL=VL
     G=(.352E19*CUR)/(E*AREA)
   4 H=G*R(J)**2.*E
     A=11.16*H
     B=2.*A*7.203E-8/(E*R(J)**2.)
     C=B*7.203E-8/(2.*E*R(J)**2.)
     D=15.7E4*G*R(J)**2.
     F=5.56E-6/R(J)
     T=DCH/VL
     IT=((T/DELT)+1.0)
     I=1
     Q(I)=0.
   5 XYZ=F*Q(I)
     IF(XYZ-87.4)9,9,7
   7 QP=A-B*Q(I)+C*Q(I)*Q(I)
```

BEST AVAILABLE COPY


```
10    COMPUTATION OF FRTO(J,K) USING AVERAGE RADII(1.5, 2.5....9.5)

      GO TO 15
    9 IF(XYZ-.00001)11,11,13
   11 QP=A-B*Q(I)+C*Q(I)*Q(I)+D
      GO TO 15
   13 QP=A-B*Q(I)+C*Q(I)*Q(I)+D*EXPF(-XYZ)
   15 I=I+1
      IF(I-1001)17,17,20
   17 Q(I)=Q(I-1)+QP*DELT
      GO TO 5
   20 T=0.
   25 T=DCH/VL
      I=(T/DELT)+1.
      Y=Q(I+1)-Q(I)
      U=I-1
      U=U*DELT
      X=T-U
      DB=Y*X/DELT
   35 QQ=Q(I)+DB
  799 DO 800 K=1,18
  798 DAC=0.
      TSTN(K)=STN(K)/VL
      TDCH=DCH/VL
      ITSTN=(TSTN(K)/DELT)+1.
      ITDCH=(TDCH/DELT)+1.
      IF(STN(K)-DCH)33,33,34
   33 DO 8000 I=1,ITSTN,2
      V(I)=1.602E-12*Q(I)*E*CUN(J)/(6.0*3.1416*1.8E-04*R(J))
 8000 DAC=DAC+(V(I)*DELT)
   88 VTER=1.602E-12*QQ*E*CUN(J)/(6.0*3.1416*1.8E-04*R(J))
  999 DAC=DAC+(VTER*X)
      FCC=DAC/SEPC
      IF(FCC-1.)800,8003,8003
   34 DO 8001 I=1,ITDCH,2
      V(I)=1.602E-12*Q(I)*E*CUN(J)/(6.0*3.1416*1.8E-04*R(J))
 8001 DAC=DAC+(V(I)*DELT)
      VTER=1.602E-12*QQ*E*CUN(J)/(6.0*3.1416*1.8E-04*R(J))
      DAC=DAC+(VTER*X)
      FCC=DAC/SEPC
      IF(FCC-1.)122,8003,8003
  122 VD=4.73E-10*QQ*ECOL*CUN(J)/R(J)
      DA=(VD)*((STN(K)-DCH)/VL)
      FC=DA/(SEP-DAC)
      FCC=FCC+((1.-FCC)*FC)
      IF(FCC-1.)800,8003,8003
 8003 FCC=1.
  800 FRTO(J,K)=FCC
      J=J+1
      IF(J-9)4,4,801
  801 DO 802 J=1,9
      DO 802 K=1,9
  802 FRTO(J,K)=FRTO(J,2*K)-FRTO(J,2*K-1)
      DO 806 J=1,9
      DO 806 K=1,9
  806 FRTO(J,K)=FRTO(J,K)*CONC(J)
      DO 803 K=1,9
      COLM(K)=0.
```

GNE/Phys/63-5

```
10    COMPUTATION OF FRTO(J,K) USING AVERAGE RADII(1.5, 2.5....9.5)

      DO 803 J=1,9
 803  COLM(K)=COLM(K)+FRTO(J,K)
      DO 804 J=1,9
      DO 804 K=1,9
 804  FRTO(J,K)=FRTO(J,K)/COLM(K)
 805  WRITE OUTPUT TAPE 3,115,((FRTO(J,K),K=1,9),J=1,9)
2000  BETA=BETA+.5
5004  WRITE OUTPUT TAPE 3,130,((XFRTO(J,K),K=1,9),J=1,9)
      CALL EXIT
      END(1,0,0,0,0,0,1,0,0,1,0,0,0,0,0)
```